PB-227 024

MATHEMATICAL MODELS OF URBAN AIR POLLUTION DYNAMICS. VOLUME III. AN URBAN HEAT ISLAND MODEL

Douglas M. Leahey, et al

New York University
New York, New York

December 1969

DISTRIBUTED BY:

NTIS

National Technical Information Service
U. S. DEPARTMENT OF COMMERCE
5285 Port Royal Road, Springfield Va. 22151

PB 227 024

New York University
School of Engineering and Science
Department of Meteorology and Oceanography
Geophysical Sciences Laboratory TR-69-11

MATHEMATICAL MODELS OF URBAN AIR POLLUTION DYNAMICS

FINAL REPORT

by

Ben Davidson
Robert Bornstein
Leonard Druyan
Douglas Leahey
Mekala Reddy
Liau-Jang Shieh
Conrad Simon

James P. Friend, Editor

VOLUME III

AN URBAN HEAT ISLAND MODEL

by

Douglas M. Leahey

Research Grant No. AP-00328-04
National Air Pollution Control Administration
United States Department of Health,
Education and Welfare

December 1969

Reproduced by
NATIONAL TECHNICAL
INFORMATION SERVICE
U S Department of Commerce
Springfield VA 22151

Table of Contents

		Page
	Acknowledgements	viii
	Abstract	ix
I.	Introduction	1
II.	Heat Exchange Processes in Urban Areas	3
	(i) Net radiation R_n	3
	(ii) Latent heat of evaporation; Q_E	5
	(iii) The conductive heat flux: Q_G	5
	(iv) Heat generated by the city; H	6
	(v) Sensible heat exchange; Q_S	7
III.	Summer's Urban Heat Island Model	9
	(i) Derivation	9
	(ii) Critical remarks	13
IV.	The Proposed Model	14
	(i) Equations for h and T within the urban heat island	14
	(ii) Definition of the urban heat island	19
	(iii) Vertical profile of potential temperature downwind of the heat island	21
	(iv) Equations for predicting T and h when the air flows into a second urban area	24
V.	The Heat Island Under Calm Conditions	27
VI.	The Air Pollution Model	28
VII.	Determination of α	29
VIII.	Values of U	30
IX.	Value of Q_{S_0}	36
X.	Sensible Heat Exchange Over Water	38
XI.	Estimates of H	39

Table of Contents (continued)

	Page
XII. Air Pollution Data	42
XIII. Results Non-Summer Cases	44
(i) The predicted pattern of T_l	44
(ii) Predicted values of h	46
(iii) Predicted values of m	50
(iv) The urban heat island under calm conditions	57
XIV. The Urban Heat Island in Summer	60
(i) Estimates of Q_{G_l}	60
(ii) Variation of m	63
XV. Conclusions	66
References	68

List of Figures

Page

Figure 1. (a) Schematic cross section of city showing build-up of adiabatic mixing layer.
(b) Successive stages in modification of stable temperature profile as air moves over an urban heat source.
(c) Corresponding successive stages in modification of vertical wind profile..... 10

Figure 2. (a) and (b) Modification of the temperature and wind profiles at a distance x from the upwind edge of the city.
(c) Coordinate system used for mathematical treatment. 12

Figure 3. (a) Idealized vertical profile of potential temperature in a column of air located within the urban heat island (solid line) and in rural areas upwind of the city (dashed line). Above the mixing layer of height h the two profiles coincide.
(b) An illustration of the identity $d\theta_1 = \alpha dh$..... 16

Figure 4. Conceptualized pattern of sensible heat exchange associated with the urban heat island phenomena. Within the transition zone there is no sensible heat exchange between the air and the ground..... 22

Figure 5. A vertical profile of potential temperature downwind of the urban heat island; h' and θ_1' are the maximum values of the height of the mixing layer and of the potential temperature that were achieved within the heat island..... 23

Figure 6. Locations of the pibal launch sites. The dashed line is the flight plan used for 16 July 1964..... 31

Figure 7. Temperature sounding made at 155th Street and Harlem River at 0625 EST, 3 May 1966. It shows a mixing layer 130 m deep. The slope of the temperature profile through the inversion is tan β..... 32

Figure 8. Average vertical profiles of the observed wind speeds for the indicated study periods..... 34

List of Figures (continued)

Page

Figure 9. Average vertical profiles of the observed wind directions for the indicated study periods..... 35

Figure 10. The 30 x 40 square mile source grid used in this study. The origin of the grid was located near The Battery which lies at the southern tip of Manhattan Island..... 37

Figure 11. Isopleths of heat release (ly/min) from domestic heating units when the air temperature is 32°F (0°C).. 41

Figure 12. Predicted isotherm pattern in the area of Manhattan Island for the period 0600-1000 EST, 10 March 1966..... 45

Figure 13. Predicted heights (m) of the elevated inversion for the period 0600-1000 EST, 10 March 1966. The wind was WSW at 3 m/sec..... 47

Figure 14. Predicted heights (m) of the elevated inversion for the period 0630-0930 EST, 16 November 1966. The wind was SE at 3 m/sec..... 48

Figure 15. A plot of the observed against the predicted inversion heights. The solid line is the theoretical one to one relation. Mean observed and predicted heights were 174 and 175 m respectively. The standard error of estimate was 30 m..... 49

Figure 16. Predicted isopleth pattern of SO_2 mixing ratio (ppm) in the area of Manhattan Island for the period 0600-1000 EST, 10 March 1966..... 51

Figure 17. Predicted isopleth pattern of SO_2 mixing ratio (ppm) in the area of Manhattan Island for the period 0630-0930 EST, 16 November 1966..... 52

Figure 18. A plot of the observed against predicted SO_2 mixing ratio. The solid line is the theoretical one to one relation..... 53

Figure 19. Observed and predicted variation of SO_2 in a NW-SE section through 79th Street, Manhattan..... 55

List of Figures (continued)

Page

Figure 20. A verification of the model against SO_2 mixing ratios observed at ground based stations. The solid line is the theoretical one to one relation..... 56

Figure 21. The distribution of the height of the elevated stable layer for the morning of 10 March 1966 following a hypothetical calm period of 2 hours duration..... 58

Figure 22. Isopleth pattern of SO_2 mixing ratio (ppm) for the morning of 10 March 1966 following a hypothetical calm period of 2 hours duration..... 59

Figure 23. Predicted isopleths of heat release (ly/min) from pavement and concrete for the period 0430-0600 EST, 16 July 1964..... 62

Figure 24. A plot of the observed against predicted inversion heights for the two summer study periods. The solid line depicts the theoretical one to one relation..... 64

Figure 25. Predicted variation of m over the New York area for the early morning of 16 July 1964..... 65

Acknowledgements

I wish to thank Professor Ben Davidson and Professor James P. Friend for their sympathetic criticisms. I am also indebted to Mrs. Lillian Bloom who did the typing and to Mrs. Gertrude Fisher who drafted the figures.

Abstract

Artificial heat sources cause the base of stable air layers which are at ground level in rural regions to become elevated over urban areas. An intervening layer characterized by an adiabatic lapse rate is formed. Within this layer pollutants are trapped and mixed in the vertical.

A model is presented for the urban heat island which is based upon the above premises and the first law of thermodynamics. It is a modified version of an advective model first advanced by Summers. The modification consists of the introduction of two heat sinks which permit an extension of the model downwind from the center of the city.

Associated with the model is a method for predicting the variation of pollution within the urban heat island. The method relates the mixing ratio of a pollutant to the thickness of the adiabatic layer.

Data collected from an instrumented helicopter have allowed extensive testing of the model for New York City. The agreements between the observed and predicted values for the depths of the mixing layer and for SO_2 mixing ratios are very encouraging. The linear correlation coefficients between the observed and predicted depths of the mixing layer and for SO_2 were .95 and .84 respectively.

The model has also permitted estimates to be made of the heat released from the pavements, asphalt and concrete of New York City. These estimates are the only quantitative values available for an urban complex.

I. Introduction

Many of the world's people live in urban areas. The influences of cities upon the atmospheric temperature structure and associated diffusion parameters are consequently of considerable concern. This is especially true in the face of increasing evidence that urban environments contribute to illness and morbidity, particularly in the case of respiratory diseases.

Of the urban meteorological influences none is so intriguing or as important as the "urban heat island" effect. The phrase was coined to describe the characteristic warmth of a city which is found during periods of light winds and nocturnal inversions. Numerous climatological studies have documented this urban induced modification of air temperatures from surface data.

Luke Howard (1833) established that London was often warmer than its environs from data collected at stations in and around London. Later similar comparisons were made from reporting stations around Paris (Renou 1862) and from St. Louis (Hammon and Duenchal 1902).

Mobile measurements from instrumented automobiles have greatly increased the quality of the data. Horizontal traverses enabled Schmit (1929) to detect sharp temperature gradients on the outskirts of Vienna. In the following years in similar studies country-city temperature differences of 14°C were found in Berlin (Reichel 1933) and 20°C in Toronto (Middleton and Millar 1936). The surface extent of the "heat island" has also been documented by Sundborg (1950), Mitchell (1962) and Chandler (1967).

The surface temperature observations have shown that:

(a) the edges of the heat island are well defined by sharp temperature gradients;

(b) across the center of the heat island the temperature gradient is relatively gentle;

(c) the center of the isotherm pattern associated with the heat island is displaced downwind from the center of the city; and

(d) parks, river banks, and other open areas are cool with temperatures similar to those found in the rural regions.

Starting with Balchin and Pye (1947) attempts were made to combine vertical and horizontal temperature measurements to determine the three-dimensional character of the heat island. Balchin and Pye studied the city of Bath, England which lies between steep hills. Observations from the hills showed that inversions existed less often over the city than over the open country. Later studies of the vertical temperature profile made with tethered kytoons (Duckworth and Sandberg, 1954), television towers (DeMarrais, 1961), and instrumented helicopter (Bornstein, 1968) have shown that inversions tend to become elevated as the air flows over an urban complex. Between the ground and the elevated inversion, the lapse of temperature is usually adiabatic or slightly stable.

The most comprehensive study of the three-dimensional aspects of the urban heat island has been made in Cincinnati, (Clarke, 1969). In addition to features documented by the previous investigators, he found a ground based stable layer downwind of the heat island. Atop this surface

layer,he detected a layer of air of near neutral stability. Finally, above this second layer, he found air whose stability was similar to that of the air upwind of the city. He considered that the neutrally stable air was flowing from the city over denser rural air. In an obvious analogy he called this outflow "the urban heat plume".

In this study, an explanation for the heat island will be advanced and verified. In addition, an undiffusive urban air pollution model based upon simple mixing layer theory will be tested. But before considering the proposed models, we will first review what is known about heat exchange processes in urban regions.

II. Heat Exchange Processes in Urban Areas

Very little is known about the components of the heat budget in urban areas. This is surprising in view of the evident importance of the heat exchange processes to urban atmospheric temperature structure. It will, however, be instructive to review the current knowledge of how urban and rural heat exchange differ.

(i) Net radiation; R_n:

The net radiation R_n at the earth-air interface may be sub-divided into short wave and long wave terms.

$$R_n = (S + s)(1 - A) + I\downarrow - I\uparrow$$

where

S = direct beam short wave radiation

s = diffuse beam short wave radiation

A = surface albedo

$I\downarrow$ = long wave radiation received by the surface from the atmosphere

$I\uparrow$ = long wave radiation emitted by the surface.

Solar radiation S+s can be attenuated by as much as 20 percent by the air pollution palls which blanket a city. Hand (1943) found that the city of Boston received on the average of 15% less solar radiation than its suburbs. A similar value for urban depletion of short wave radiation has recently been reported for the Montreal area (East, 1968). This value is also in agreement with the theoretical values of depletion that one might expect as a result of pollution (Blackwell, et al., 1954).

Changes of albedo from field and forest to asphalt, slate and stone are small. An airborne survey by Kung, Bryson and Lenschow (1964) showed that urban albedo values are about 10% lower than rural albedos. Seasonal variations dependent upon snow cover and foliage can be expected.

Pollutants in the urban atmosphere intercept and re-radiate long wave radiation groundward. From theoretical calculations Sheppard (1958) estimated that as a result of pollutant emissions long wave radiation received at the ground in the city can exceed that received in rural areas by more than 10 percent. Reliable observations concerning the quantitative effects of pollution upon the sky radiation $I\downarrow$ are, however, scarce (Fuggle and Oke (1968)). Despite this lack of data, the nocturnal urban heat island as Berljand (1968) pointed out, has often been ascribed to the attenuation of long wave radiation by urban aerosols.

There is also a dearth of knowledge about $I\uparrow$. One might specu-

late that the long wave radiation emitted by the earth's surface would be greater in the "warm" cities than in rural areas. Munn (1966), however, cautions that interception by vertical buildings could complicate the behavior of this component.

(ii) Latent heat of evaporation; Q_E:

Urban areas are characterized by impervious surfaces of roofs and streets. Rain water is rapidly drained off these surfaces so when precipitation ceases only thin films remain to be evaporated. This is in contrast to rural areas where soil and vegetation store large quantities of water which subsequently evaporate slowly. On the average, because of the more readily available moisture, evaporative heat loss Q_E, will probably be greater in rural areas.

The problem is complicated by the release of water vapor through combustion processes. In the winter, for example, when vapor pressures in rural areas are usually low, domestic heating units are putting moisture into the urban atmosphere. During this period the humidity over cities can exceed that over neighboring rural areas (Kratzer, 1956). Chandler (1967) further shows from data collected in Leicester, England that during summer nights vapor pressures in towns may be greater than in rural areas. Usually, however, cities possess lower absolute and relative humidities than rural area (Chandler, 1965).

(iii) The conductive heat flux; Q_G:

The pavements and concrete surfaces of a city have relatively high heat capacities and heat conductivities. As a result, the city is able

to store larger quantities of solar radiation than rural areas. Decreased evaporational cooling also results in larger amounts of heat being stored in the city's fabric.

Because of the higher daytime storages of solar energy the release of heat from the ground at night should be greater in urban areas than in rural areas. One would expect this difference in heat flux from the ground to be a maximum in the summer, when solar radiation is greatest, and a minimum during the winter when solar radiation is least.

The behavior of the conductive heat flux in urban areas can be discussed only in a qualitative manner. There are no suggestions of its magnitude in the literature.

(iv) Heat generated by the city; H:

Domestic heating units and industrial activities release large quantities of heat into the air. During the winter months this energy release H, can become a dominant term in the heat budget. Bornstein (1968) has estimated that in downtown Manhattan heat released from artificial heat sources during January is typically 2.5 times the energy received from the sun.

Davidson (1967) compiled a unique detailed inventory of the yearly amount of fuel consumed by industries and housing units for a 1200 square mile area centered on New York City. These fuel data will be used in this study to provide estimates of the heat generated by the city and its neighboring towns.

(v) Sensible heat exchange; Q_S:

The sensible heat exchange from the air to the ground Q_S, is dependent through the heat budget equation upon the behavior of R_n, Q_E, Q_G and H. We will restrict our attention to mornings when the air is characterized by a ground based stable layer upwind of the city.

Consider the heat budget equation for a rural area:

$$(S_0 + s_0)(1 - A_0) + I_0\downarrow - \sigma T_0^4 = \pm Q_{G_0} \pm Q_{E_0} - Q_{S_0} \qquad (1)$$

and for a location in which there is an artificial heat source.

$$(S_1 + s_1)(1 - A_1) + I_1\downarrow - \sigma T_1^4 = \pm Q_{G_1} \pm Q_{E_1} \pm Q_{S_1} - H \qquad (2)$$

The subscripts 0 and 1 refer to rural and non-rural areas respectively. An upward transfer of Q_E or Q_S according to sign convection is positive while for Q_G and H the reverse is true, with a downward flow being positive.

In these equations we have assumed that the Stefan-Boltzmann law for radiating black bodies is valid.

i.e.

$$I\uparrow = \sigma T^4$$

where

σ = Stefan-Boltzmann constant

T = temperature of the ground (°A).

We will further assume

(1) that the larger sky radiation $I_1^{\downarrow}$ over a city is sufficient to compensate for the depletion in short wave radiation heat flux so that

$$I_1^{\downarrow} - I_0^{\downarrow} = (S_0 + s_0)(1 - A_0) - (S_1 + s_1)(1 - A_1)$$

and (2) that the exchange of latent heat in the rural and urban areas are the same, i.e.

$$Q_{E_0} = Q_{E_1}.$$

Then by subtracting (2) from (1).

$$Q_{S_1} = H \pm (Q_{G_1} - Q_{G_0}) - \sigma(T_1^4 - T_0^4) - Q_{S_0}.$$

In the non-summer months $Q_{G_1} \approx Q_{G_0}$. Hence

$$Q_{S_1} \approx H - \sigma(T_1^4 - T_0^4) - Q_{S_0}. \qquad (3)$$

During the summer mornings H is small, the flux from the ground is upward and $Q_{G_1} >> Q_{G_0}$. Hence

$$Q_{S_1} \approx Q_{G_1} - \sigma(T_1^4 - T_0^4) - Q_{S_0}. \qquad (4)$$

The behavior of Q_{S_1} as deduced from equations (3) and (4) will be used to explain the urban heat island phenomena.

III. Summer's Urban Heat Island Model

Summers (1965) has proposed a simple heat island model and considered its application to air pollution problems. Because his model was the inspiration for the present study, his derivation will be given and then critically appraised.

(i) Derivation

Summers considered a layer of stable air upwind of a city in which the lapse rate is less than the dry adiabatic Γ by an amount α_0. As the air gains heat in its passage over the city thermal turbulence creates a mixing layer characterized by an adiabatic lapse rate and the base of the stable layer rises. These concepts are illustrated in Figures 1a and 1b.

The vertical profile of wind will also be influenced by the thermal turbulence. Summers assumed that the mean wind in a mixing layer of height h must equal the mean wind up to the same height in the country. As the air in the adiabatic layer is being mixed by thermal forces it will tend to have a uniform wind with height. Based upon these assumptions the wind profile will be modified in a manner shown in Figure 1c.

If the surface temperature of the air at a distance x into the city is T_x and the depth of the mixing layer is h the following relations hold

$$T = T_0 - (\Gamma - \alpha_0)\, h$$

and

$$T = T_x - \Gamma h$$

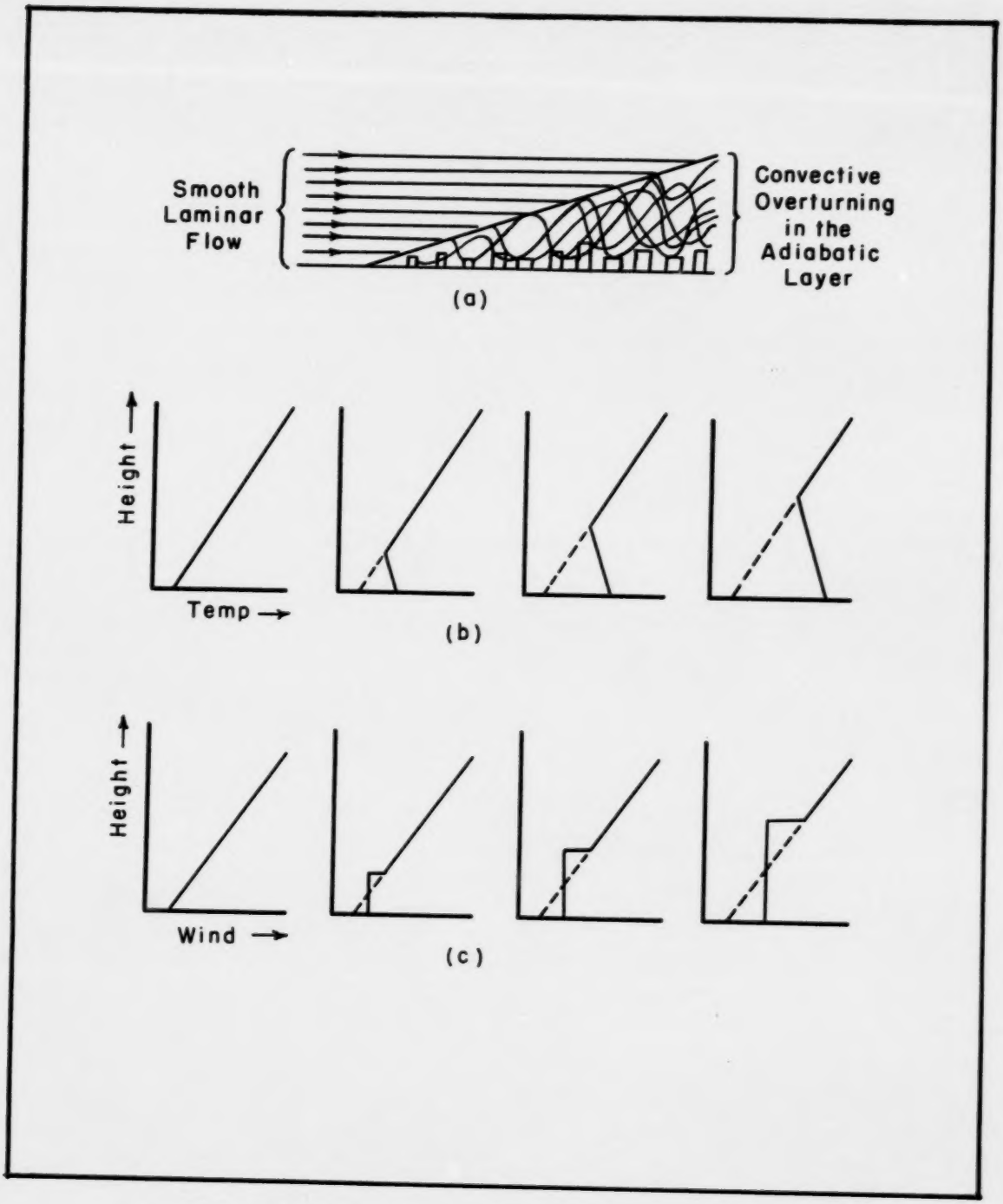

Figure 1. (a) Schematic cross section of city showing build-up of adiabatic mixing layer.
(b) Successive stages in modification of stable temperature profile as air moves over an urban heat source.
(c) Corresponding successive stages in modification of vertical wind profile.

where T_0 and T are the temperatures at the surface in the country and at the bottom of the elevated stable layer respectively (Figure 2a). Solving these two equations for T_x he got

$$T_x = T_0 + \alpha_0 h \tag{5}$$

Now assume the wind in the rural area increases linearly with height,

$$U = U_0 + bz .$$

Then in accordance with Summers assumptions the mean wind $\overline{U}$ in the mixing layer will be

$$\overline{U} = U_0 + \frac{bh}{2} .$$

Because the lapse rate within the mixing layer is adiabatic the potential temperature has a constant value equal to T_x throughout the layer. Summers states that the total heat B_x passing through a vertical cross section of width Δy and height h (see Figure 2c) in unit time is

$$B_x = \rho c_p \Delta y T_x \left(U_0 + \frac{bh}{2}\right) h, \tag{6}$$

where

ρ = density of air

and c_p = specific heat of air.

In the country the potential temperature at height z is $T_0 + \alpha_0 z$ and the amount of heat B_0 passing through a cross section of height h in unit time is

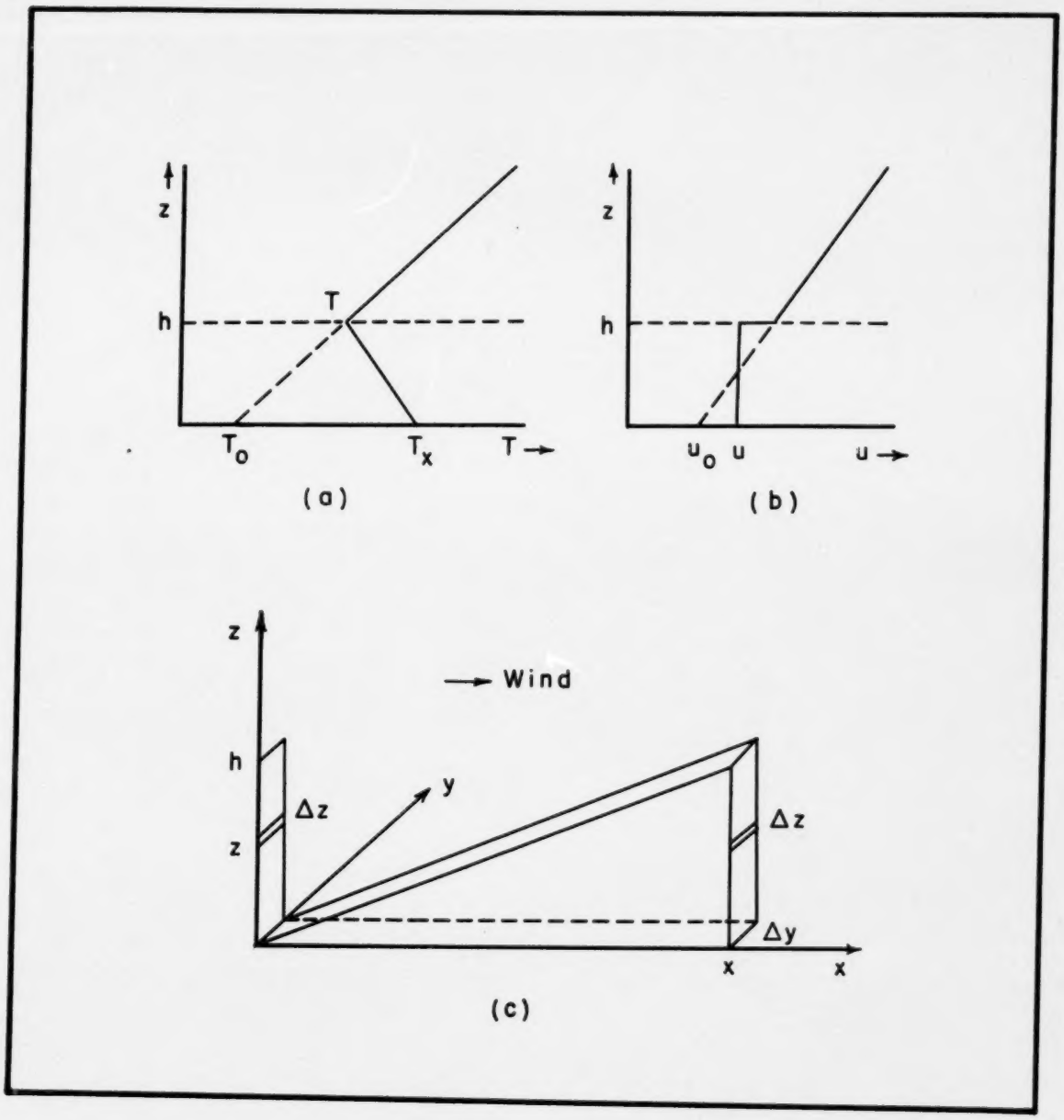

Figure 2. (a) and (b) Modification of the temperature and wind profiles at a distance x from the upwind edge of the city.
(c) Coordinate system used for mathematical treatment.

$$B_0 = \rho c_p \Delta y \int_0^h (U_0 + bz)(T_0 + \alpha_0 z)\, dz. \qquad (7)$$

Performing this integration and subtracting the result from (6) Summers got the total heat gained between the two cross sections in unit time.

$$B_x - B_0 = \rho c_p \Delta y \alpha_0 h^2 \left(\frac{U_0}{2} + \frac{bh}{6} \right). \qquad (8)$$

Now if the heat output of the city at distance x from its edge is $H(x)$ cal cm^{-2} sec^{-1}, the total output between the two cross sections per unit time is

$$\Delta y \int_0^x H(x)\, dx,$$

where $x = 0$ is the upwind edge of the city. Thus, from equation (8)

$$h^2 \left(U_0 + \frac{bh}{3} \right) = \frac{2}{\alpha_0 \rho c_p} \int_0^x H(x)\, dx. \qquad (9)$$

This last equation together with equation (5) forms the basis of Summers heat island model. Although Summers lacked the detailed data needed to test it, he was able to show that it yields values of h which are of the correct magnitude.

(ii) Critical remarks

(a) The origin of equations (6) and (7) is obscure. It can be shown from the first law of thermodynamics that Summers has made two unstated though justifiable assumptions. Namely, that air behaves as an ideal gas and that the ratio of the temperature to the potential temperature

of the air approximates unity.

(b) Summers does not define what he means by the "upwind edge" of the city. This definition is important as observations show that the heat island effect is apparent only after the air penetrates some distance into the suburbs.

(c) Implicite in equation (9) is the assumption that all the heat generated by a city is given as sensible heat to the air. Summers considered that the effect of heat sinks such as $-Q_{S_0}$ and $-\sigma (T_1^4 - T_0^4)$ of equations (3) and (4) were negligible. It will be shown however that the inclusion of these sinks helps to better our understanding of the urban heat island effect.

(d) Summers model does not predict the temperature decrease downwind of an urban complex. Because of this limitation Summers restricts the use of his model to upwind portions of a city.

(e) Summers model does not permit the calculation of mixing depths when $U = 0$.

IV. The Proposed Model

Summers idea of explaining the urban heat island effect by means of a simple advective thermodynamic model can be enlarged through the inclusion of heat sinks. The introduction of these sinks will provide a basis for defining the urban heat islandand will permit a logical extension of the model downwind from the center of the city.

(i) Equations for h and T within the urban heat island

As a column of stable air moves from the country into the city,

thermal turbulence causes an adiabatic lapse rate to form from the ground to a height h. Above this height the vertical gradient of potential temperature, α, is the same as one would encounter in rural areas upwind of the city. Thus, within a column of air located in a city one would find two vertical gradients of potential temperature. These are shown in Figure 3. A change in the potential temperature of the mixed layer $d\theta_1$ will be related to a change in depth of that layer, dh, by the equation

$$d\theta_1 = \alpha \, dh. \tag{10}$$

If the atmosphere is assumed to be an ideal gas one can show from the first law of thermodynamics that

$$\bar{\partial} H = c_p \frac{T}{\theta} \, d\theta, \tag{11}$$

where

$\bar{\partial}H$ = an infinitesimal amount of heat added to the air per unit mass (cal/kg °K)

c_p = specific heat of air at constant pressure (cal/kg °K)

T = temperature of the air (°K)

and θ = potential temperature of the air

Within the first 400 meters of the earth's surface, the region to which we are directing our attention $\frac{T}{\theta} = 1$ to a very good approximation. Making use of this fact in equation (11) we get

$$\bar{\partial} H = c_p \, d\theta. \tag{12}$$

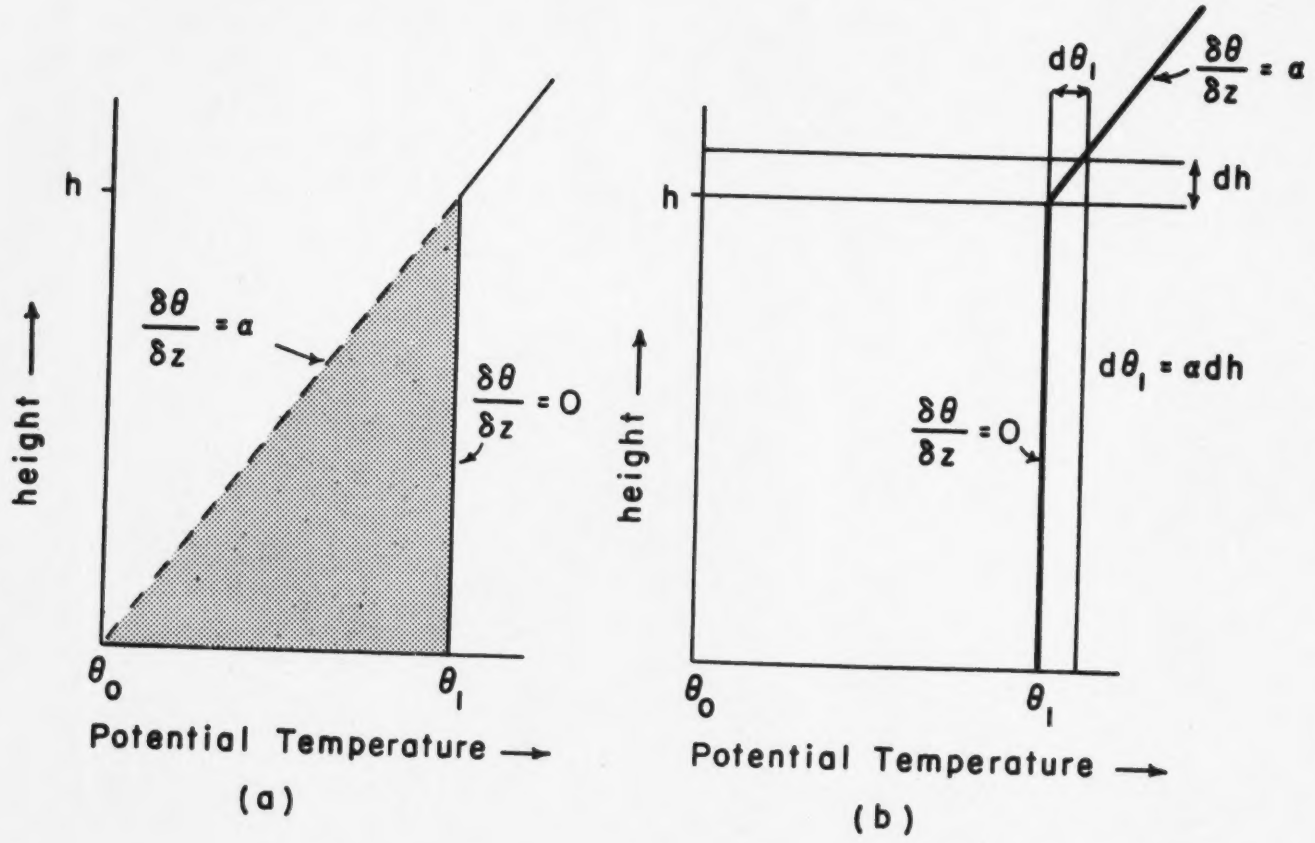

Figure 3. (a) Idealized vertical profile of potential temperature in a column of air located within the urban heat island (solid line) and in rural areas upwind of the city (dashed line). Above the mixing layer of height h the two profiles coincide.
(b) An illustration of the identity $d\theta_1 = \alpha dh$.

Within the mixing layer where we know that $d\theta = d\theta_1 = \alpha\, dh$ equation (12) becomes

$$\bar{\partial}H = c_p\, \alpha\, dh.$$

If we multiply both sides of this equation by ρh we get

$$\rho h\, \bar{\partial}H = c_p \rho\, \alpha\, h\, dh, \tag{13}$$

where ρ = air density (kg/m^3) and is assumed to be a constant.

The quantity $\rho h \bar{\partial}H$ is the amount of heat added to a column of air of unit cross sectional area and height h, provided one assumes that this additional heat is uniformly distributed within the column. It must equal

$$Q_{S_1}\, dt$$

where Q_{S_1} = the rate at which sensible heat is gained (cal/m^2 sec) by the air column through its lower face,

and dt = the time increment over which the column receives the sensible heat, Q_{S_1}.

We can now assume that

$$dt = \frac{dx}{U}$$

where dx = the distance (m) over which the column acquires the heat $\rho h \bar{\partial}H$

and U = wind speed (m/sec). It is assumed constant with height.

This relation enables one to write equation (13) as

$$c_p \rho\, \alpha\, h\, dh = \frac{Q_{S_1}}{U}\, dx$$

or integrating and rearranging terms:

$$\frac{\alpha h^2}{2} = \frac{1}{c_p \rho} \int_{x_1}^{x} \frac{Q_{S_1}}{U} \, dx \qquad (14)$$

where x_1 = the distance along the column's trajectory at which Q_{S_1} first becomes positive. As can be verified by inspection the right hand side of the above equation is equal to the shaded area of Figure 3. Finally, by assuming that U does not vary in time or space we obtain

$$h^2 = \frac{2}{c_p \rho U \alpha} \int_{x_1}^{x} Q_{S_1} \, dx. \qquad (15)$$

This equation is similar to Summers expression for h, when there is no wind shear upwind of the city (i.e. b = 0).

Equation (10) can be integrated to yield

$$\theta_1 = \theta_o + \alpha h$$

where θ_o = potential temperature at the surface in the rural area upwind of the city. By definition the potential and actual temperatures are the same at the earth's surface. Therefore

$$T_1 = T_o + \alpha h. \qquad (16)$$

Equations (15) and (16) provide the means of predicting depths of the mixing layer and surface temperatures within the urban heat island.

(ii) Definition of the urban heat island

We arenow in a position to propose a definition for the urban heat island.

Observations show that mixing layers are associated with urban heat islands. But according to equation (14) mixing layers develop only when Q_{S_1} is positive. The expression for Q_{S_1} during non-summer months from equation (3) is

$$Q_{S_1} = H - \sigma(T_1^4 - T_0^4) - Q_{S_0}. \qquad (3)$$

Upwind from the city $0 \leq H < Q_{S_0}$, Q_{S_1} is negative and the flow of heat is from the atmosphere to the ground. As the air passes through the suburbs this downward heat flow becomes less until a transition zone is reached in which the exchange of sensible heat between the atmosphere and the ground is zero. The heat island effect of a city becomes noticeable beyond this transitional zone where H exceeds Q_{S_0} resulting in a net gain of heat by the air. When this happens a mixing layer of depth h forms and from equation (15)

$$h^2 = \frac{2}{U \alpha c_p \rho} \int_{x_1}^{x} \left(H - \sigma(T_1^4 - T_0^4) - Q_{S_0}\right) dx. \qquad (17)$$

This relation together with equation (16) can be solved for h and T_1 to a desired degree of accuracy by iteration methods.

As the air moves downwind from the city its surface temperature

increases to a maximum T_1'. At this juncture H is balanced by the sink terms. Another transition zone is reached in which Q_{S_1} is zero.

Beyond this transition zone the heat exchange processes must be postulated. Any postulations will necessarily have a degree of arbitrariness. But there are three restrictions which should be recognized.

(1) Equation (3) must be satisfied, i.e.

$$Q_{S_1} = H - \sigma(T_1^4 - T_0^4) - Q_{S_0}. \qquad (3)$$

(2) The turbulent heat flux in the air column before it reaches the transition zone is from the ground to the air. It should take a finite time for this eddy heat flux to reverse its direction. In recognition of this plausibility, it seems reasonable to assume the existence of a finite region in which Q_{S_1} is zero.

(3) To accord with observations the model should permit the surface temperatures downwind of the urban heat island to be similar to those upwind.

The following proposed sequence of heat exchange satisfies these three requirements.

(a) In the second transition zone where $Q_{S_1} = 0$

$$\sigma(T_1^4 - T_0^4) = H - Q_{S_0}, \quad H > Q_{S_0}.$$

It will be assumed that on the average the transition zone ends when $H = Q_{S_0}$ at which point $T_1 = T_0$.

(b) Beyond the transition zone equation (3) is satisfied by a loss of sensible heat to the ground and

$$Q_{S_1} = H - Q_{S_0} \qquad H < Q_{S_0}.$$

Thus, in rural areas downwind from the city where H = 0, $Q_{S_1} = - Q_{S_0}$.

Besides accounting for the "cool" temperatures found downwind of an urban complex this postulated pattern of heat exchange also accounts for "cool" temperatures found in parks and other open areas within a city. Formerly tentative explanations for the "cool" temperatures have been based upon hypothesized local wind circulations between rural and urban areas (Clarke, 1969), between the heat island and the suburbs (Munn, 1966) and between parks and built up areas (Kratzer, 1956, Whiten, 1956).

A schematic representation of the postulated pattern of sensible heat exchange is given in Figure 4. The positive quality of Q_{S_1} between the transition zones comprises the defining characteristic of the urban heat island.

So far the discussion has been limited to non-summer months. Through the use of equation (4) rather than equation (3) the discussion can be extended by obvious analogy to include summer months.

(iii) Vertical profile of potential temperature downwind of the heat island

Shown in Figure 5 is a vertical profile of potential temperature downwind of the city consistent with the postulated pattern of heat exchange. The magnitude of the gradient of potential temperature near the ground can-

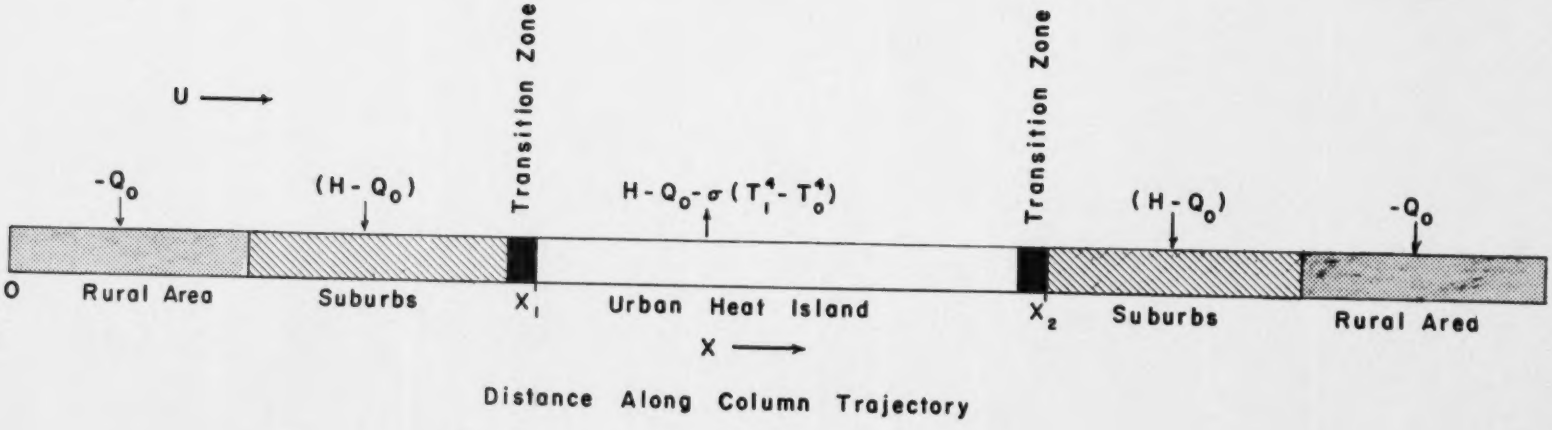

Figure 4. Conceptualized pattern of sensible heat exchange associated with the urban heat island phenomena. Within the transition zone there is no sensible heat exchange between the air and the ground.

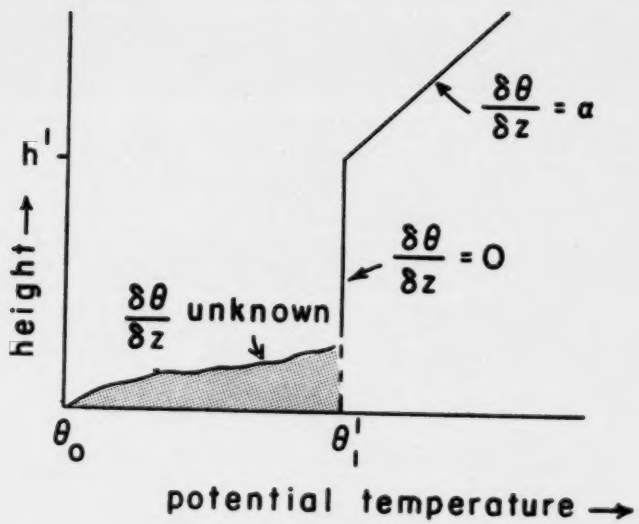

Figure 5. A vertical profile of potential temperature downwind of the urban heat island; h' and θ'_1 are the maximum values of the height of the mixing layer and of the potential temperature that were achieved within the heat island.

not be deduced from the present theory. The area of the shaded portion A, however, can be related to the heat loss, by the equation

$$A = \frac{1}{c_p \rho U} \int_{x_2}^{x} (Q_{S_0} - H)\, dx, \quad H < Q_{S_0}, \qquad (18)$$

where x_2 is the distance along the trajectory at which $H = Q_{S_0}$. The arguments justifying equation (18) are similar to the ones used for equation (14).

As previously mentioned, Clarke found that temperature soundings taken downwind of Cincinnati, Ohio displayed the features shown in Figure 5. He hypothesized, however, that the stable air next to the ground had originated from rural areas downwind of the city.

(iv) Equations for predicting T and h when the air flows into a second urban area.

Having passed from an urban into a rural area the air may from thence pass through a third transitional zone into another urban area. This third transitional zone will lie in the region where the heat lost by the air in the intercity portion of the trajectory exceeds the heat gained from the second urban area. That is in the region where

$$\int_{x_3}^{x} [H - \sigma (T_2^4 - T_0^4) - Q_{S_0}]\, dx < \int_{x_2}^{x_3} (Q_{S_0} - H)\, dx.$$

Here

x = the full length of the air column's trajectory

x_3 = the distance along the trajectory at which artificial heating from the second urban area first exceeds Q_{S_0},

T_2 = the ground temperature within the second urban area beyond $x = x_3$

x_2 = the distance along the trajectory at which one leaves the transition zone downwind of the first urban heat island (see Figure 4).

There are presently neither theory nor observations from which one might infer the general behavior of $\frac{\partial \theta}{\partial z}$ in the intercity region. Because of this lack of knowledge one cannot apply our mixing layer theory to predict the behavior of T_2 within the third transitional zone. But one can show that when the second urban area has supplied the air with an amount of sensible heat equal to that lost in the intercity region $T_2 = T_1'$. In recognition of this and also of the fact that $T_2 = T_0$ upwind of $x = x_3$ it is proposed to use the following weighted temperature difference to estimate T_2 within the third transitional zone.

$$T_1 = T_0 + \frac{\left[\int_{x_3}^{x} (H - \sigma(T_2^4 - T_0^4) - Q_{S_0})\, dx\right](T_1' - T_0)}{\int_{x_2}^{x_3} (Q_{S_0} - H)\, dz} \qquad (19)$$

Beyond the point where $T_2 = T_1'$ one can show that

$$T_2 = T_0 + \alpha h_2$$

where

$$h_2^2 = h'^2 + \frac{2}{c_p \rho U \alpha} \int_{x_4}^{x} (H - \sigma(T_2^4 - T_0^4) - Q_{S_0})\, dx$$

h' = maximum value of the height of the mixing layer achieved within the first urban heat island

x_4 = the distance along the trajectory at which $T_2 = T_1'$.

Problems will arise where one might wish to have estimates for the depth of the mixing layer within the third transitional zone. Following the type of argument which resulted in equation (19), we are led to propose the use of the following equation

$$h_2 = \frac{\int_{x_3}^{x} (H - \sigma(T_2^4 - T_0^4) - Q_{S_0})\, dx \; [h']}{\int_{x_2}^{x_3} (Q_{S_0} - H)\, dx} \qquad (20)$$

This equation ensures that the following requirements be met:

(1) $h_2 = 0$ at $x = x_3$

and (2) $h_2 = h'$ at $x = x_4$.

Equations (19) and (20) are used for expedient reasons. The need to employ the type of argument which served for their justification highlights the deficiencies of our model. But calculations performed by the author which will be presented later in this paper have shown that third type transitional zones will usually occupy only very small portions of a given air trajectory. As a result, the portion of the urban heat island calculations contaminated by estimates such as those contained in equations (19) and (20) will be minimal.

V. The Heat Island Under Calm Conditions

In the special case when the air is calm (U = 0), the model appears to predict a mixing layer of infinite depth. But this is not physically possible. We will recall the derivation of equation (15) to resolve the paradox.

In deriving equation (15) we assumed that

$$dt = \frac{dx}{U}.$$

When U = 0 this assumption is no longer valid and we must retain the original expression

$$c_p \rho \alpha h \, dh = Q_{S_1} \, dt.$$

Or integrating and using the identity for Q_{S_1}

$$h^2 = \frac{2}{c_p \rho \alpha} \int_0^t (H - \sigma(T_1^4 - T_0^4) - Q_{S_0}) \, dt + h_0^2 \qquad (21)$$

where

t = the time over which the calm persists and

h_0 = the depth of the mixing layer at t = 0.

From this last equation one sees that the mixing layer will continue to grow under calm conditions until the sink terms balance the source term. That is until such time as

$$\sigma T_1^4 = H - Q_{S_0} - \sigma T_0^4 .$$

VI. The Air Pollution Model

Within the mixing layer thermal turbulence tends to cause the pollutants to become homogeneously distributed in the vertical. Following Summers, we will assume homogeneity and use it to link our heat island model to the spatial variation of air pollution.

A frequently used air pollution parameter is the mixing ratio, m, defined as the mass of pollutant per unit mass of dry air in the mixture. Thus

$$m = \frac{\rho_P}{\rho} \tag{22}$$

where

ρ_P is the concentration of pollutant (mass per unit volume).

In a column of air with cross section ΔA and of height h the concentration of the uniformly distributed pollutant is given by the relation

$$\rho_P = \frac{P}{h\Delta A} \tag{23}$$

where P is the total mass of the pollutant in the column. In steady state conditions where the wind velocity is constant with height for a column of unit cross section

$$P = \int_0^x \frac{Q_P \, dx}{U} . \tag{24}$$

Where Q_P is the amount of pollutant emitted by the city (kg/m^2 sec) along the trajectory of the column. With unit cross sectional area equations (22), (23) and (24) yield

$$m = \int_0^x \frac{Q_P \, dx}{U h \rho} \, . \qquad (25)$$

As with mixing depth calculation one must make an exception for the case when $U = 0$. Again in this circumstance one cannot use the relation $dt = \frac{dx}{U}$. In a straightforward derivation similar to that which resulted in equation (25) it can be shown that

$$m = \frac{m_0 h_0}{h} + \int_0^t \frac{Q_P \, dt}{h \rho} , \qquad (26)$$

where

m_0 = the mixing ratio of the pollutant at $t = 0$

t = the time over which the calm persists.

The height h employed in equations (25) and (26) can be calculated by means discussed in the previous section. Predictions based upon equations (25) and (26) can thus provide implicit verification of the heat island model.

VII. Determination of α

Davidson (1967) has described in detail the measurement techniques and instruments used in New York University's Urban Air Pollution Dynamics Study. Most of the data analyzed in this paper were collected as part of that project. For one study period (22 June 1966) the temperature soundings were collected as part of a project sponsored by Consolidated Edison Company (Simon, 1968).

Temperature and SO_2 data were collected by an instrumented helicopter which made vertical soundings and horizontal traverses in the New York metropolitan area. A typical flight plan is shown in Figure 6. Seven of the mornings for which soundings are available were characterized by an identifiable stable layer located near the ground.

These urban temperature soundings were used to obtain α. The procedure is illustrated in Figure 7. Near the ground the vertical gradient of potential temperature is related to the slope of the temperature profile through the stable layer, tan β, by the equation

$$\alpha = \tan \beta - \Gamma$$

where Γ is the adiabatic lapse rate.

A value of α was determined from each of the profiles used in a particular study period. The α's were then averaged and the result employed in the calculation.

VIII. Values of U

Wind data were obtained from 45 g lift pilot balloons released at one or more of the following stations (see Figure 6): Pelham Manor (PM), New York University (NYU), Research Building No. 4 (RB), Welfare Island (WI) and Great Kills (GK). Wind speed and direction were averaged in the vertical from the surface to 400 m. An average of the winds obtained in this manner for each site was then employed in the calculations.

The number of "pibal" flights available for this averaging varied with the study period. Listed in Table I are the study periods together with

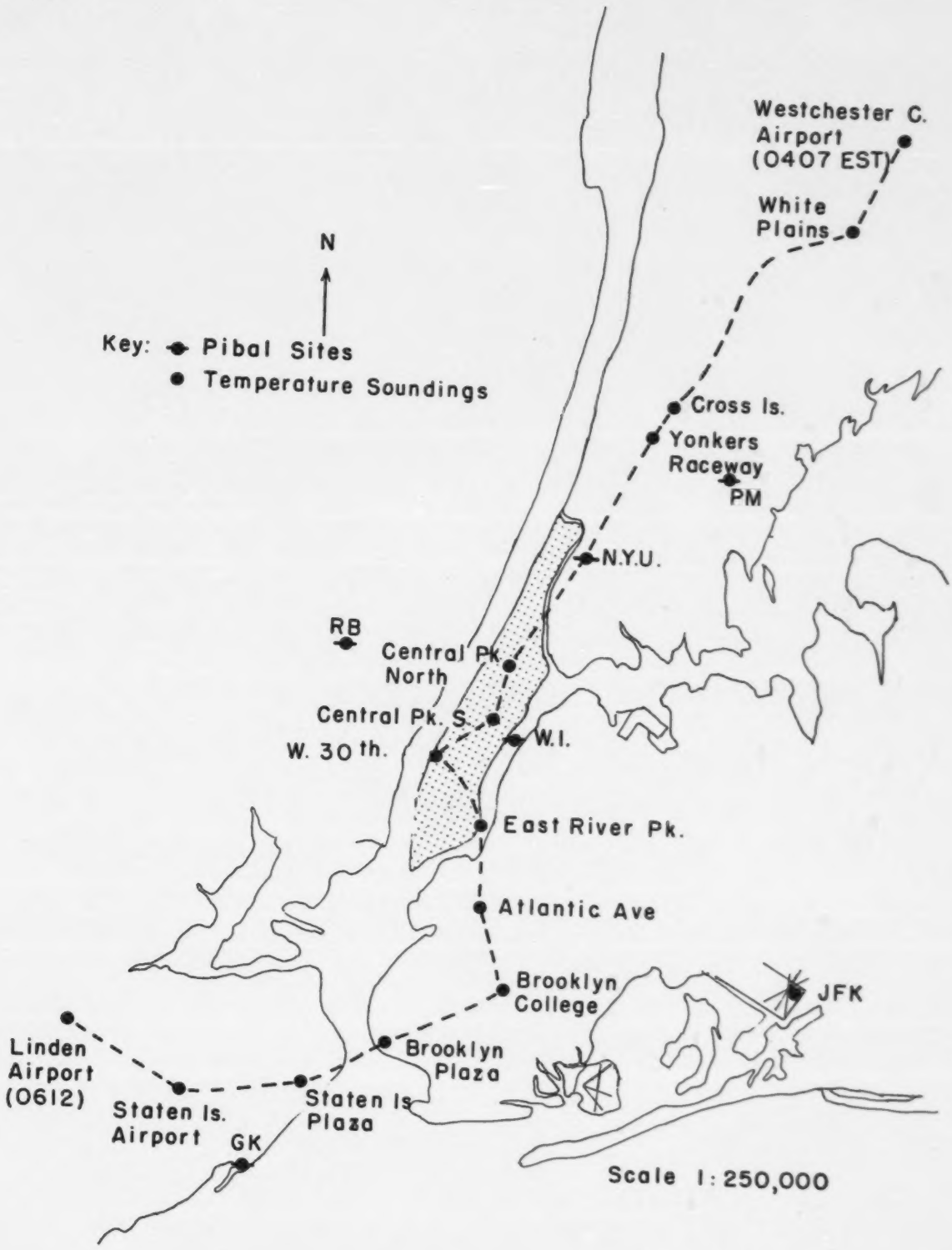

Figure 6. Locations of the pibal launch sites. The dashed line is the flight plan used for 16 July 1964.

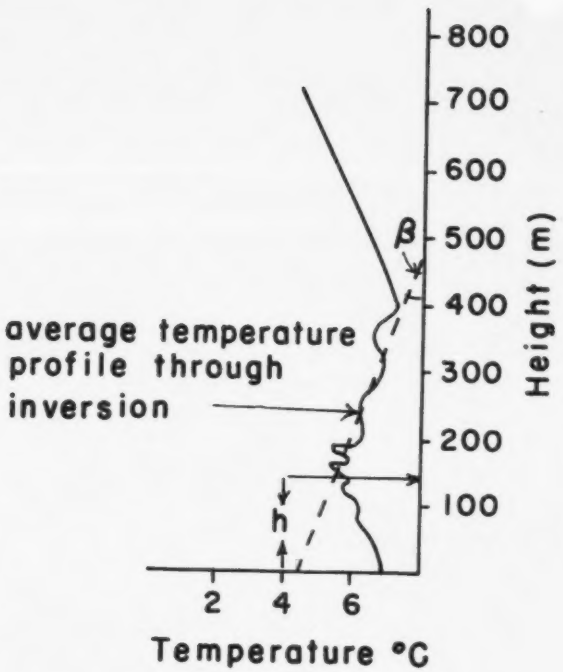

Figure 7. Temperature sounding made at 155th Street and Harlem River at 0625 EST, 3 May 1966. It shows a mixing layer 130 m deep. The slope of the temperature profile through the inversion is tan β.

the number and location of associated pibal flights.

Table I. Pilot balloon flights

Study Period (EST)	Location					
	PM	NYU	RB	WI	GK	Total
16 July 1964, 0430-0600	4		4		4	12
9 March 1966, 0630-0900			4	1		5
10 March 1966, 0600-1000		4	3			7
11 March 1966, 0630-0730		2	2			4
3 May 1966, 0600-0700	1					1
22 June 1966, 0430-0630						--
16 November 1966, 0630-0930	2			3		5

Pibal data were not available for the 22 June 1966. For this period the wind speed and direction were obtained from surface observations made at Central Park.

The assumption is made in the theory that wind velocity is invariant with height. It is of interest therefore to inquire how this assumption agrees with the observed wind profiles. Figures 8 and 9 show the vertical profiles of the average wind speed and direction. For the 9 March and 16 July periods the assumption appears to be very good. During the other periods the observed velocity increased appreciably with height and tended to veer. The plotted profiles for 3 May depart most noticeably from the assumed conditions. They are based, however, on data from only one balloon observation (Table I).

Displayed in Table II is the derived wind information together with the appropriate values of T_0 and α for each study period.

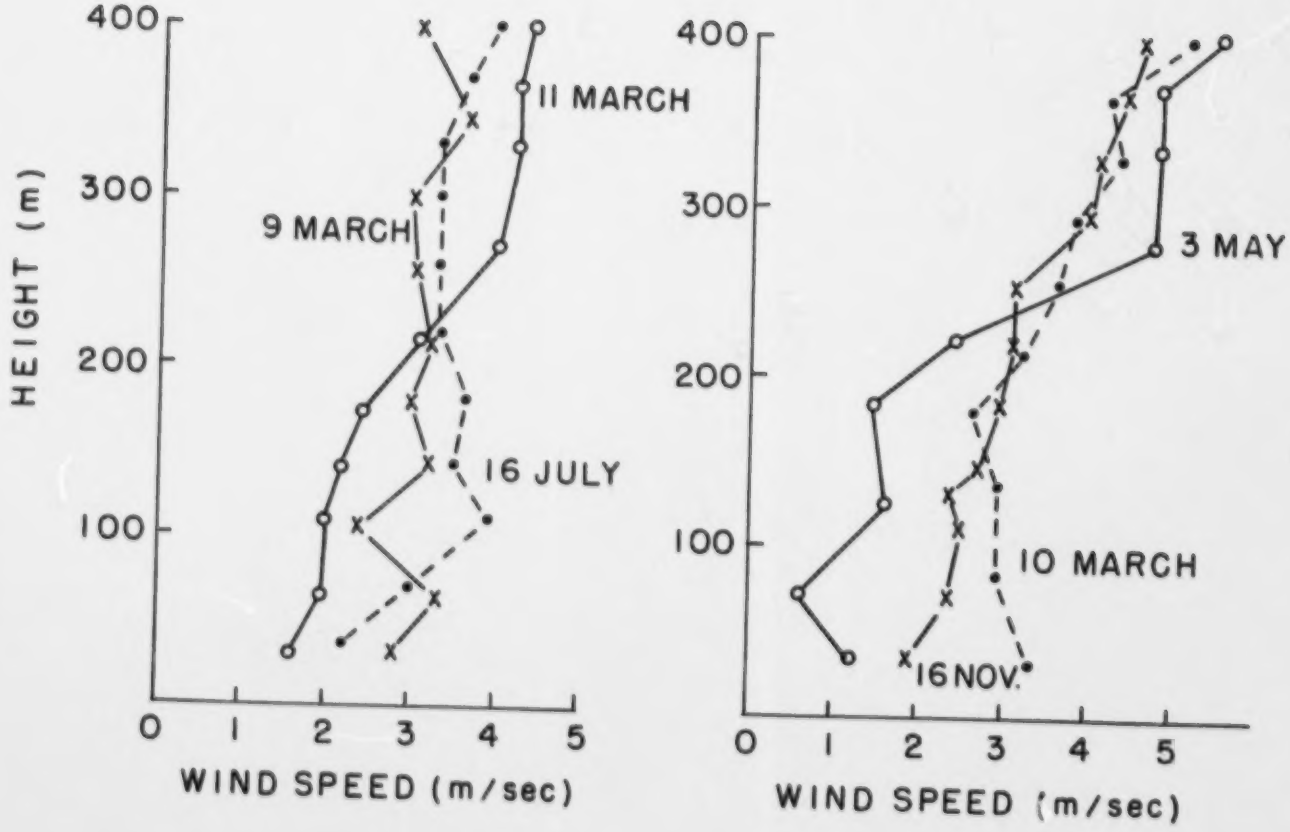

Figure 8. Average vertical profiles of the observed wind speeds for the indicated study periods.

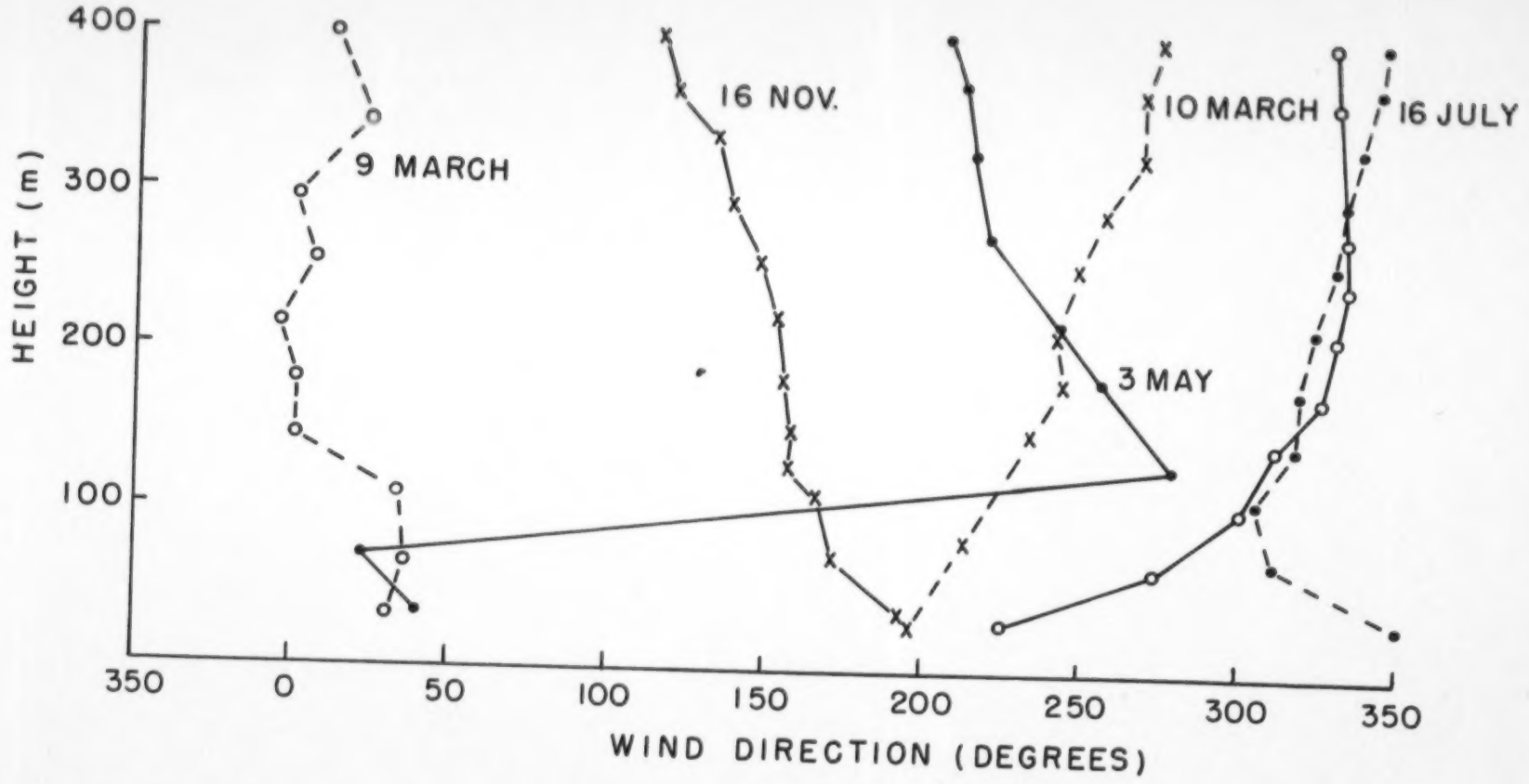

Figure 9. Average vertical profiles of the observed wind directions for the indicated study periods.

Table II. Values of T_0, α and U.

Time (EST)	T_0(°C)	α(°C/100 m)	U	
			Direction (deg)	Speed (m/sec)
16 July 1964				
0430-0600	21.0	1.00	330	3.4
	21.0	1.00	330	3.4
9 March 1966				
0630-0800	-5.0	1.35	10	3.0
0800-0900	-5.0	0.75	10	3.0
10 March 1966				
0600-1000	0.0	1.76	250	3.5
11 March 1966				
0630-0730	5.0	2.00	330	3.0
3 May 1966				
0600-0700	7.0	1.70	190	3.0
22 June 1966				
0430-0600	17.0	1.00	40	5.8
16 November 1966				
0630-0930	2.0	.66	150	3.1

With the wind speeds given in Table II, a column of air will take up to ten hours to traverse the study area shown in Figure 10.

IX. Value of Q_{S_0}

As direct measurements of Q_{S_0} were not available resort was made to the gradient equation

$$Q_{S_0} = c_p \rho K \frac{\partial \theta}{\partial z}$$

or

$$Q_{S_0} = c_p \rho K \alpha$$

where K (cm^2/sec) is the coefficient of eddy heat conduction.

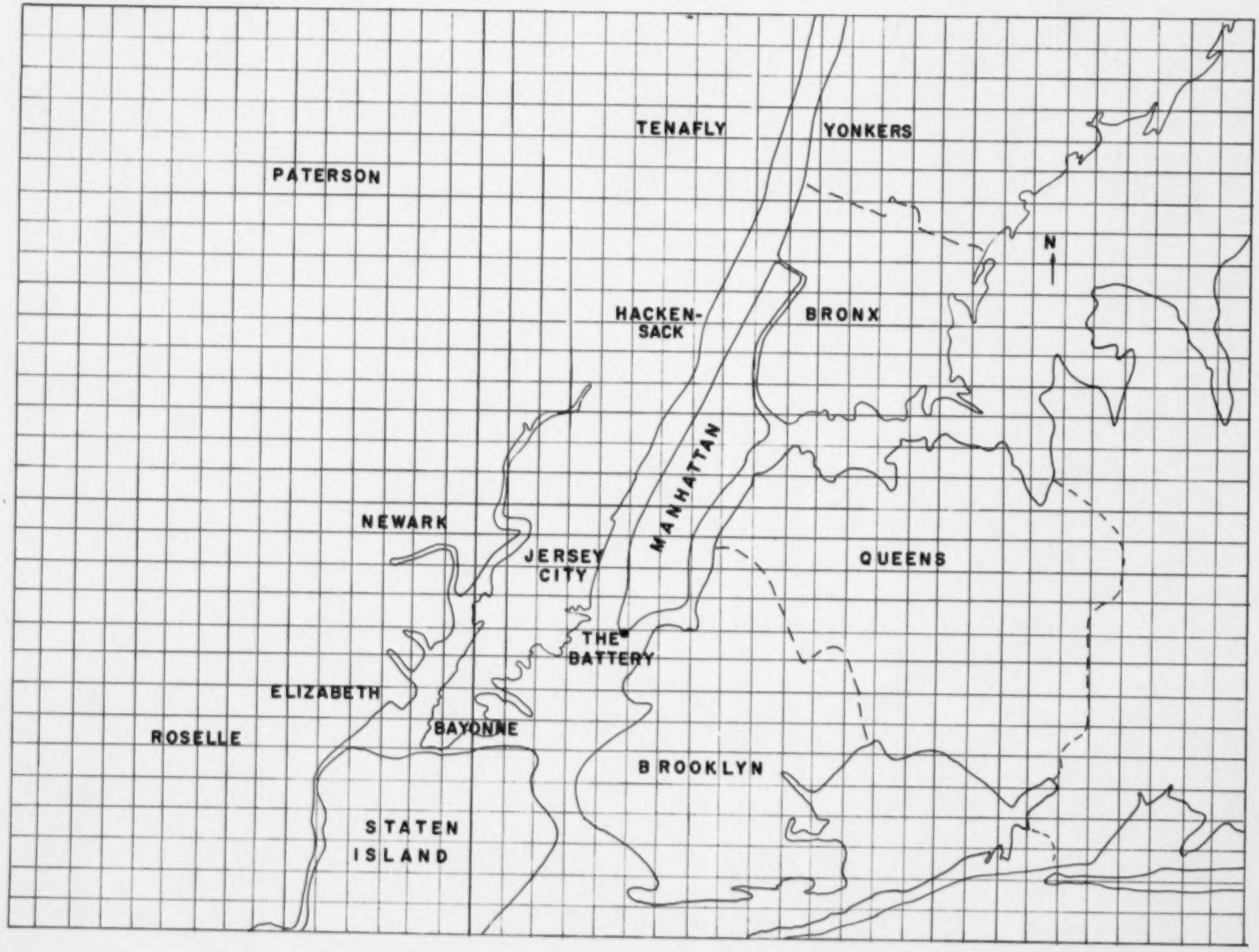

Figure 10. The 30 x 40 square mile source grid used in this study. The origin of the grid was located near The Battery which lies at the southern tip of Manhattan Island.

Under stable conditions Haltiner and Martin (1957) suggest $K = 5 \times 10^3 \text{ cm}^2/\text{sec}$. The average of all the α's used in this paper (Table II) is 1.37°C/100 m. With this value for α the calculated Q_{S_0} is -.013 ly/min.

Gradient equations at best are accurate only to orders of magnitude. With this in mind it was decided to accept the above value of Q_{S_0} without alteration for all study periods.

X. Sensible Heat Exchange Over Water

Air blowing over New York City encounters the Hudson, East and Harlem Rivers. These water bodies can have a marked influence upon the ambient temperature structure. This is especially true when the air which passes over them is colder. Under such circumstances the air gains sensible heat with a consequential enhancement of the heat island effect.

Following Vowinckel and Taylor (1965) formulae devised by Shuleiken (1953) were used to calculate sensible heat fluxes from the water surfaces.

For water warmer than air $Q_S = 30.24 (T_w - T_l)$.

For water colder than air $Q_S = .226 U (T_w - T_l)$.

where Q_S = sensible heat flux (cal/cm^2 day).

T_l = temperature of the air (°C).

T_w = temperature of the water (°C).

U = wind speed (m/sec).

Water temperatures have been measured off the southern end of Manhattan Island since 1927 and climatological monthly means are available

from the U.S. Department of Commerce (1960). These temperature data were used in the above formulae.

XI. Estimates of H

Estimates of the amount and types of domestic fuel consumed per square mile in a 30 x 40 square mile grid centered on New York City (Figure 10) were made by Messrs. Ingram, Kaiser and Simon. G. Hoffnagle compiled an inventory of the yearly amount and types of fuel consumed by power plants, hospitals and by 170 of the largest industries in the study area. The New York City Department of Traffic has provided estimates of the amount of vehicular fuel burned on a daily basis in each square mile of the city's five boroughs. Similar data for every county included in this study has been published by the U.S. Department of Health, Education and Welfare (1967). From these data average areal rates of heat release (cal/m^2 sec) and of SO_2 emissions (kg/m^2 sec) can be calculated.

There are two major components of H

$$H = H_1 + H_2$$

where

H_1 = rate at which heat produced for domestic needs is conducted to the atmosphere from buildings. It is temperature dependent and will be the largest component during non-summer months.

H_2 = the rate at which heat is given to the atmosphere as the result of vehicular traffic and industrial activities. It should be constant throughout the year.

Fuel burnt in residential units and hospitals is used for space heating, cooking, and heating hot water. The percentage of the annual fuel used for the last two items may be significant. Estimates range from 10% in the rural regions to 30% on Manhattan Island. But to a first approximation all the annual fuel consumption was considered to be distributed according to heating degree days. Thus,

$$H_1 = \frac{Db}{a}(65 - T_1^0) \qquad (26)$$

where

H_1 = the average rate of heat release (cal/m^2 sec) for the square mile being considered

D = the annual amount of heat release from residential units in that square mile (cal/year)

T_1^0 = the air temperature (°F), $T_1^0 < 65$ °F

a = the average number of heating degree days for New York City (4871 °F/year)

b = a conversion factor which makes the equation dimensionally correct.

Equation (26) is generally accepted by civil engineers and is widely employed. Displayed in Figure 11 in a Cartesian coordinate system, whose origin is at The Battery, are isopleths of H_1 (ly/min) on a day when T_1^0 = 32 °F. The maximum amount of heat release (.31y/min) is more than 2.5 times the .1141y/min London (1957) calculated as reaching the surface from the sun in January.

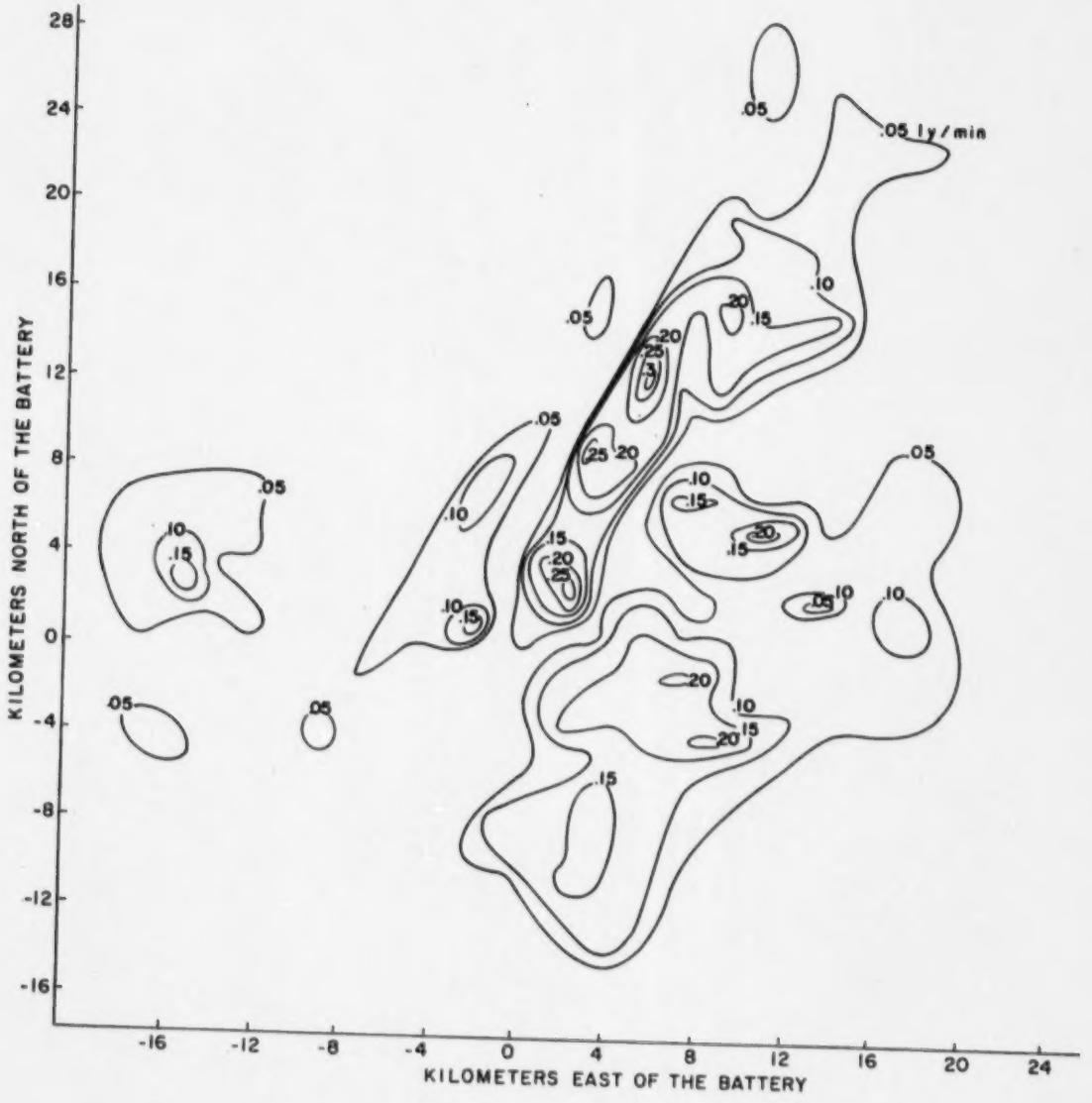

Figure 11. Isopleths of heat release (ly/min) from domestic heating units when the air temperature is 32°F (0°C).

The available estimates of the daily amount of vehicular fuel burnt within the study area were employed to calculate the heat release due to automobiles. Data for the percentage of the daily traffic which crosses Manhattan Bridges for each hour from 7 to 11 A.M. are available from New York's Traffic Department. These data were assumed to be indicative of the morning traffic pattern over the entire study area. Average heat releases due to vehicles were found to be less than .01 ly/min. Individual estimates per square mile seldom exceeded .02 ly/min.

A knowledge of the yearly amount of fuel consumed by industries and power plants were used with the following assumptions to estimate their contributions to the city's artificial heating.

(1) Manufacturing companies work a 40 hour week.

(2) Chemical companies work a 60 hour week.

(3) Power plant activity is evenly distributed throughout the year.

(4) Fifty percent of all heat released by industries and power plants is given to the air. The remainder of the heat is used by the manufacturing and chemical processes or is given to the Hudson River or other bodies of water. These first order approximations permitted an easy assessment of the heat released by industries and power plants.

Each square mile of the grid system was assumed to be an area heat source the strength of which was found by adding the components of H.

XII. Air Pollution Data

Sulfur dioxide was selected as the convenient pollutant for testing the air pollution model. Residential units, industries and power plants are the chief sources of this pollutant. Gasoline is essentially free of sulfur so

vehicular traffic is not an important SO_2 source in the New York City area. (It is a principle source of SO_2 in Los Angeles, where however concentrations are less than .01 ppm).

Estimates of SO_2 emission rates were made from the same data which yielded estimates of heat release. As in the case of heat, SO_2 released from hospitals and housing units was assumed dependent upon the number of degree days. The SO_2 released by industries and power plants were estimated on the basis of the assumptions listed in the previous section.

Some power plants have high stacks through which SO_2 and other gases are emitted with large exit velocities. As a result, these power plant plumes often penetrate the elevated inversion and are not trapped within the mixing layer. Simon (1968) has done a study of penetration of inversions by plumes from Consolidated Edison plants in New York City. In conformance with his findings the following simple concept of plume rise was adopted: the SO_2 from power plants is assumed to be trapped in the mixing layer if $h > 300$ m, otherwise it is assumed to penetrate into the inversion layer. An exception to these assumptions was made for the Ravenswood plant which has particularly high stacks with large exit velocities. For this plant the critical height for the mixing layer was taken to be 400 m.

All SO_2 sources including power plants were treated as part of an area source. No provision was made for emission by point sources.

Mixing ratios of SO_2 over the New York City area were determined from helicopters equipped with a minaturized continuously recording Davis instrument. Mobile measurements of SO_2 mixing ratios were made from similarly instrumented automobiles. In addition, data from nine ground sites maintained by New York City were utilized in the analysis.

Occasionally the helicopter flew from the mixing layer into the inversion layer in its horizontal traverses or made sorties near smoke stacks through undiffused plumes. Some subjectivity was therefore allowed in rejecting SO_2 data that appeared inconsistent with nearby observations. As a result nearly 6 percent of the helicopter data was considered unrepresentative.

XIII. Results Non-Summer Cases

(i) The predicted pattern of T_1

Data from the five non-summer study periods listed in Table II were examined. The stable layer was assumed to be ground based at the upwind edges of the study area (Figure 10). Calculations of the height of the elevated stable layer and of ground temperatures were then made every mile on a grid which was oriented parallel with the wind.

Displayed in Figure 12 are isotherms which show the predicted heat island effects on surface temperature for the period 0600-1000 EST 10 March 1966. The wind was south-westerly at 3.5 m/sec. The heat island effects due to the cities of Newark, Elizabeth, Bayonne, Jersey City, Manhattan and the Bronx are all discernible. Three features are noteworthy:

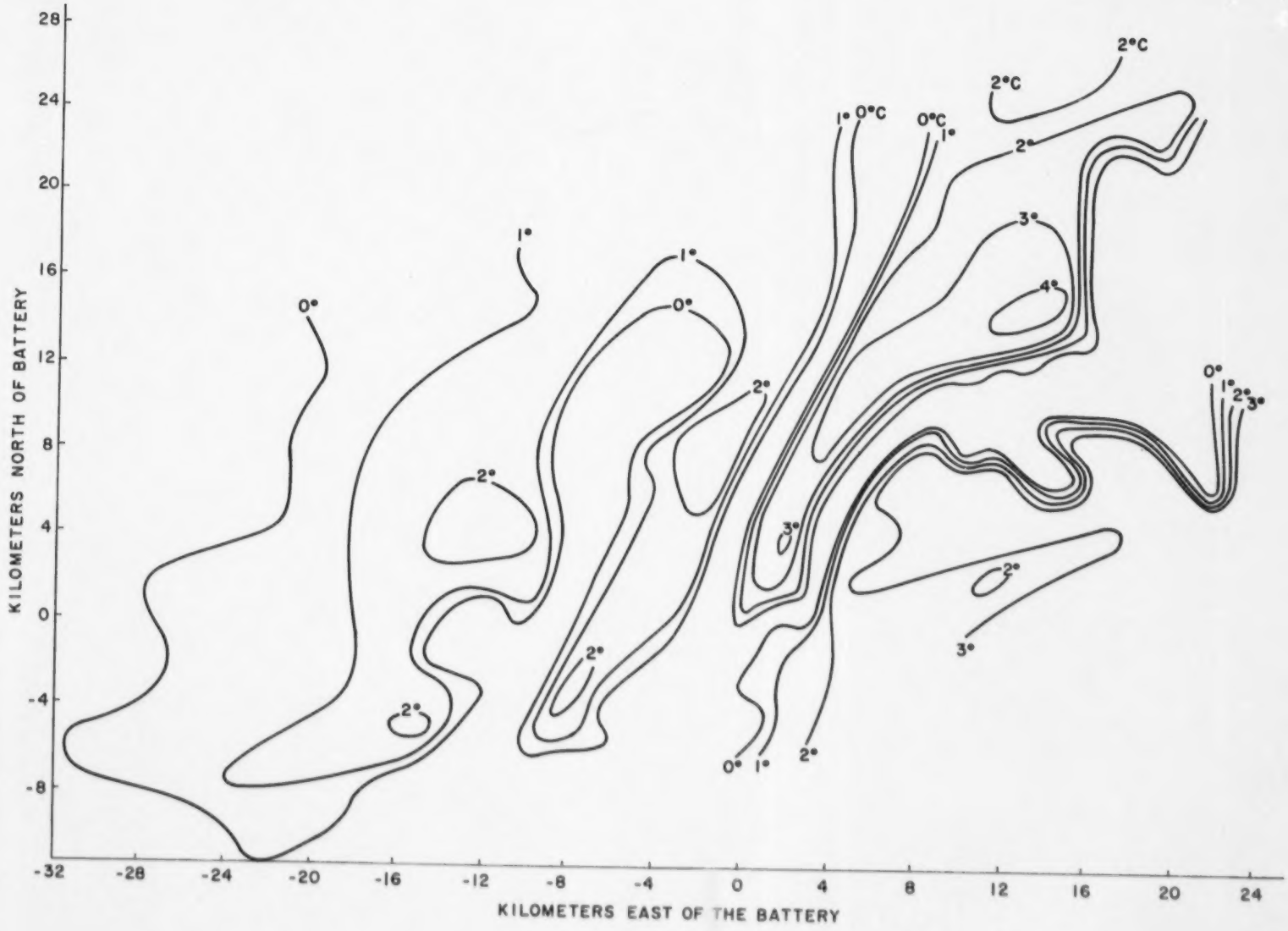

Figure 12. Predicted isotherm pattern in the area of Manhattan Island for the period 0600-1000 EST, 10 March 1966.

(1) The edges of the heat island are well defined. This is especially true of the downwind edge.

(2) The temperature gradient across the center of the heat island is relatively gentle.

(3) The center of the isotherm pattern is displayed downwind from the center of maximum heat input. This feature is most noticeable in the isotherm pattern associated with Manhattan and the Bronx. Here the greatest heat input is over Manhattan and the western Bronx (Figure 11) but the warmest temperatures are found in the eastern Bronx.

These three features are characteristic of the observed surface temperature distributions associated with urban heat islands.

(ii) Predicted values of h

Displayed in Figure 13 are the predicted depths of the mixing layer for the same time period as Figure 12. The wind is south-westerly and the gradients of h are relatively small. The base of the stable layer is shown as remaining below 250 m. Shown in Figure 14 is the distribution of h for the 16 November study period. In this figure the wind is south-easterly, height gradients are large and the base of the inversion rises to over 350 m. The thicker mixing layer is primarily due to the smaller value of α (Table II).

The agreement between predicted and observed mixing depths for each of the five periods is displayed in Figure 15. The substantial agreement is reflected in the linear correlation coefficient of .95. Further agreement between the predicted and observed inversion heights is presented in Table III.

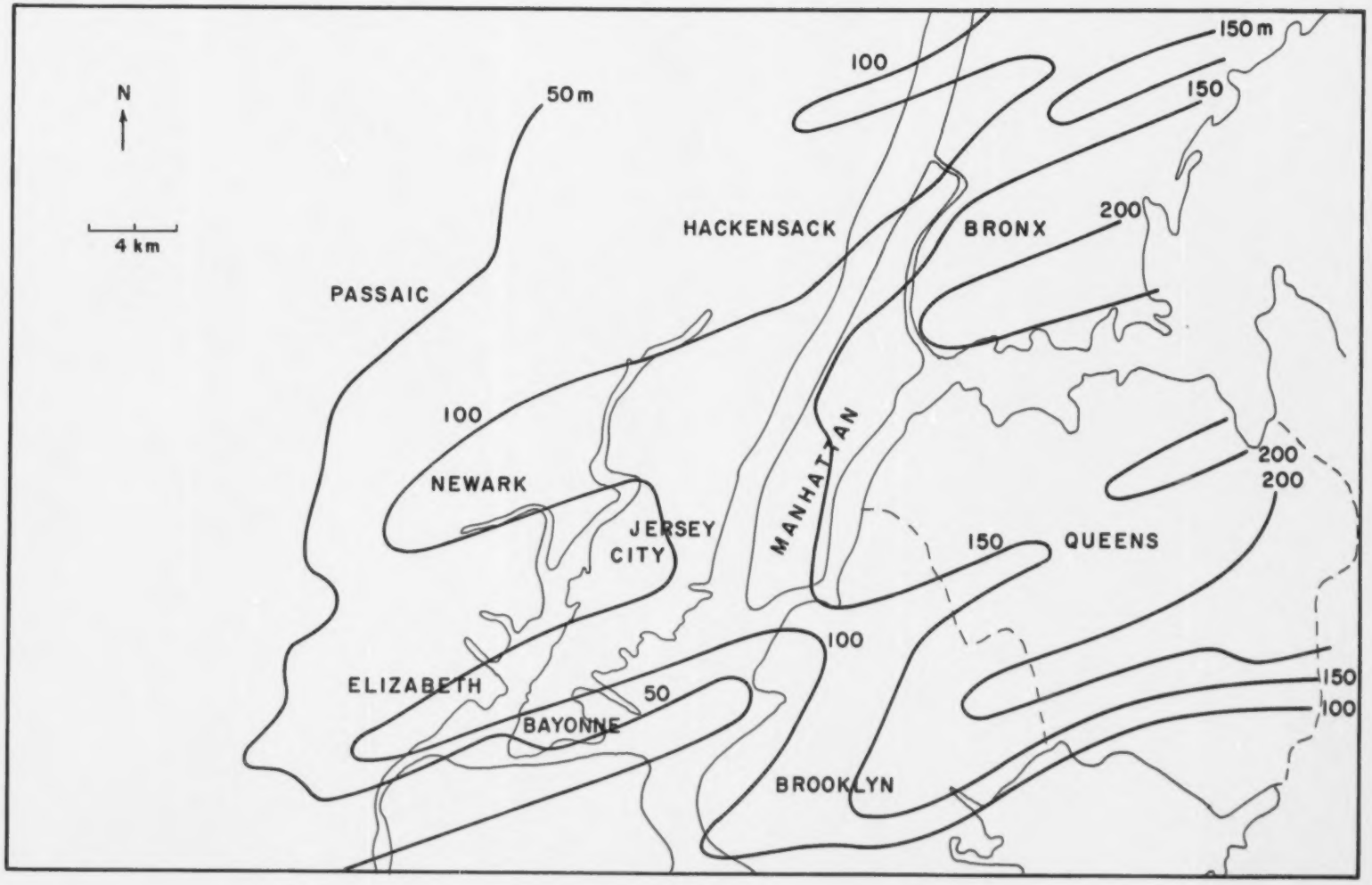

Figure 13. Predicted heights (m) of the elevated inversion for the period 0600-1000 EST, 10 March 1966. The wind was WSW at 3 m/sec.

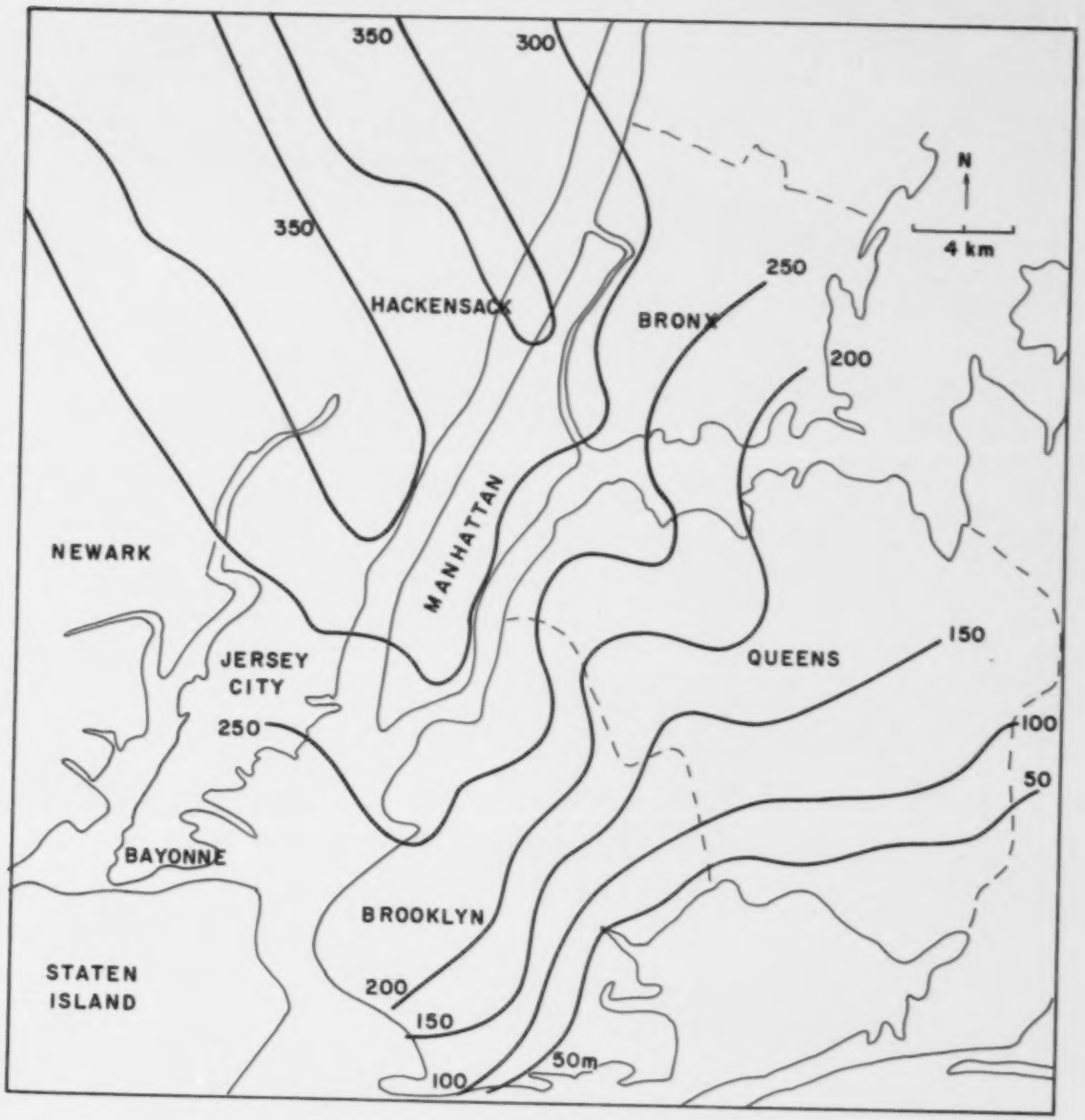

Figure 14. Predicted heights (m) of the elevated inversion for the period 0630-0930 EST, 16 November 1966. The wind was SE at 3 m/sec.

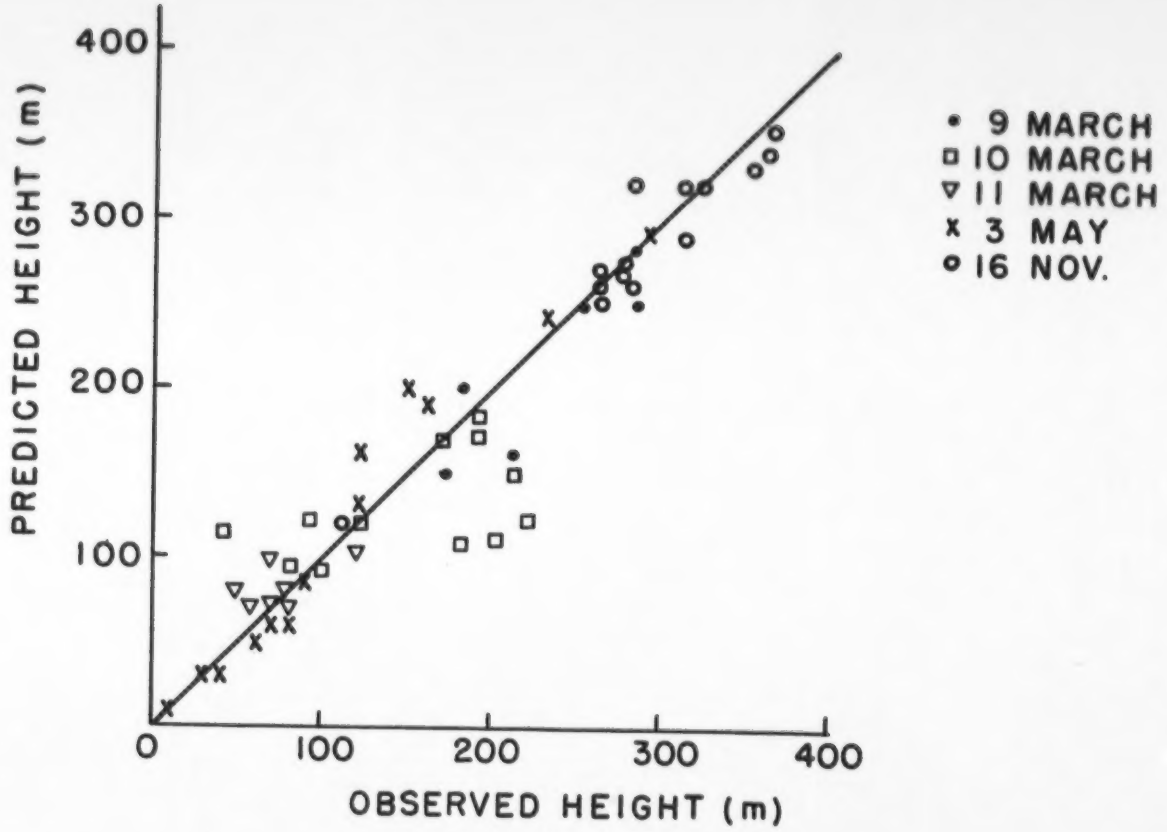

Figure 15. A plot of the observed against the predicted inversion heights. The solid line is the theoretical one to one relation. Mean observed and predicted heights were 174 and 175 m respectively. The standard error of estimate was 30 m.

Table III. Comparison between observed and predicted values of h.

Morning Period	Number of Soundings	Mean Observed h(m)	Mean Predicted h(m)	Standard Error (m)
9 March 1966	6	215	228	26
10 March 1966	12	151	133	52
11 March 1966	7	76	81	18
3 May 1966	13	111	118	21
16 November 1966	14	286	288	15
Total	52	174	175	30

(iii) Predicted values of m

Calculations for the distribution of SO_2 across the study area were made from equation (25). Figure 16 shows predicted isopleths of m in parts per million (ppm) for the 10 March study period. Very high values of m are predicted downwind of Manhattan Island. As plumes from utilities were assumed to be penetrating into the stable layer ($h < 300$ m) by far the greatest portion of this pollution is due to domestic heating. Isopleths of m for the 16 November study period are given in Figure 17. The fingers of high pollution predicted to the west of Manhattan Island are caused by power plant plumes which are trapped within the mixing layer ($h > 300$ m).

Both Figures 16 and 17 illustrate that the simple advective model predicts maximum pollution concentration downwind of a city. This is in contrast to air pollution models based on the diffusion equation (e.g. Turner, 1967) which associate areas of maximum pollution with the major sources of emissions.

Figure 18 shows a plot of the predicted values of m against the observed values. The observed values come from an instrumented helicop-

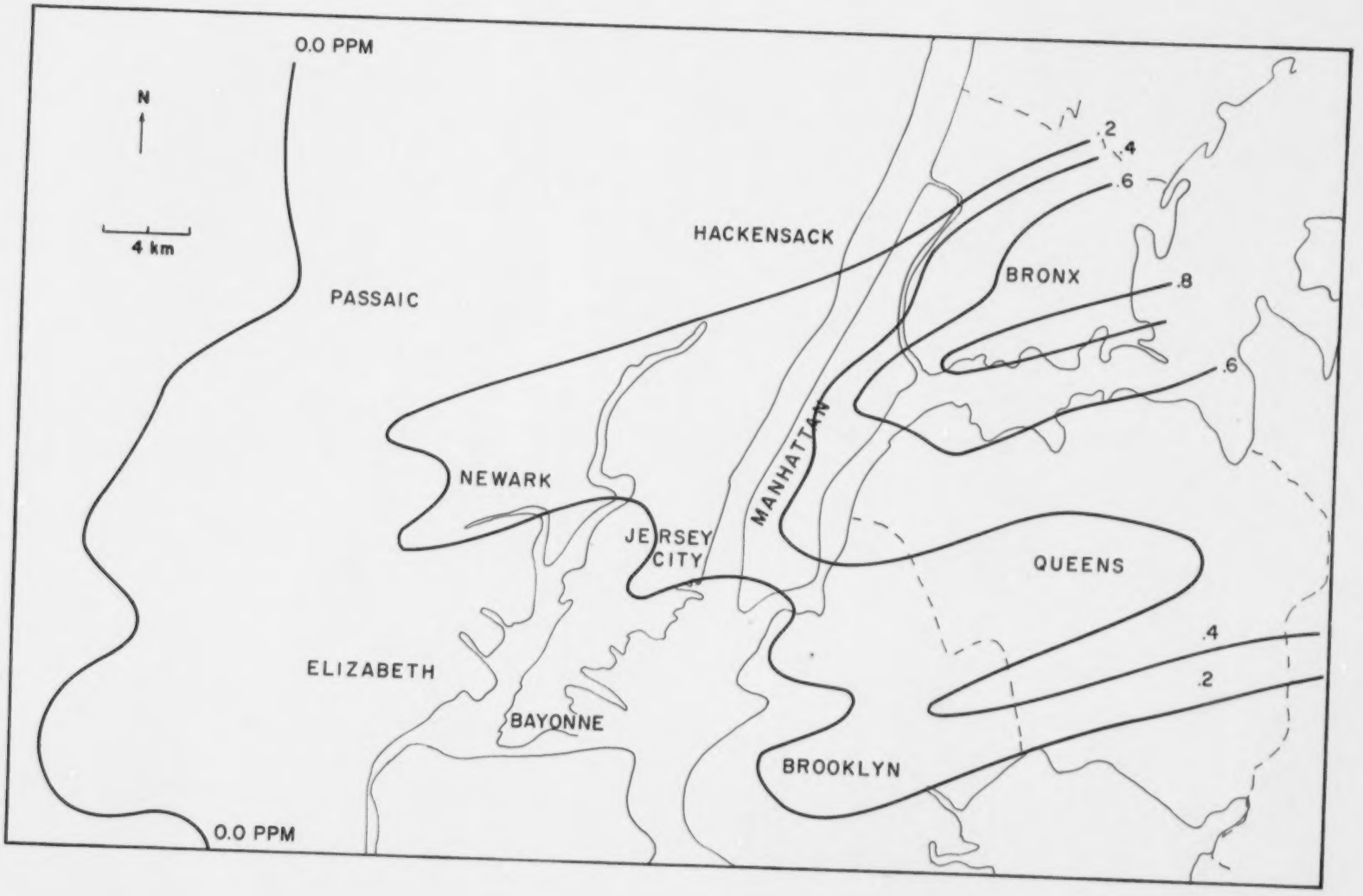

Figure 16. Predicted isopleth pattern of SO_2 mixing ratio (ppm) in the area of Manhattan Island for the period 0600-1000 EST, 10 March 1966.

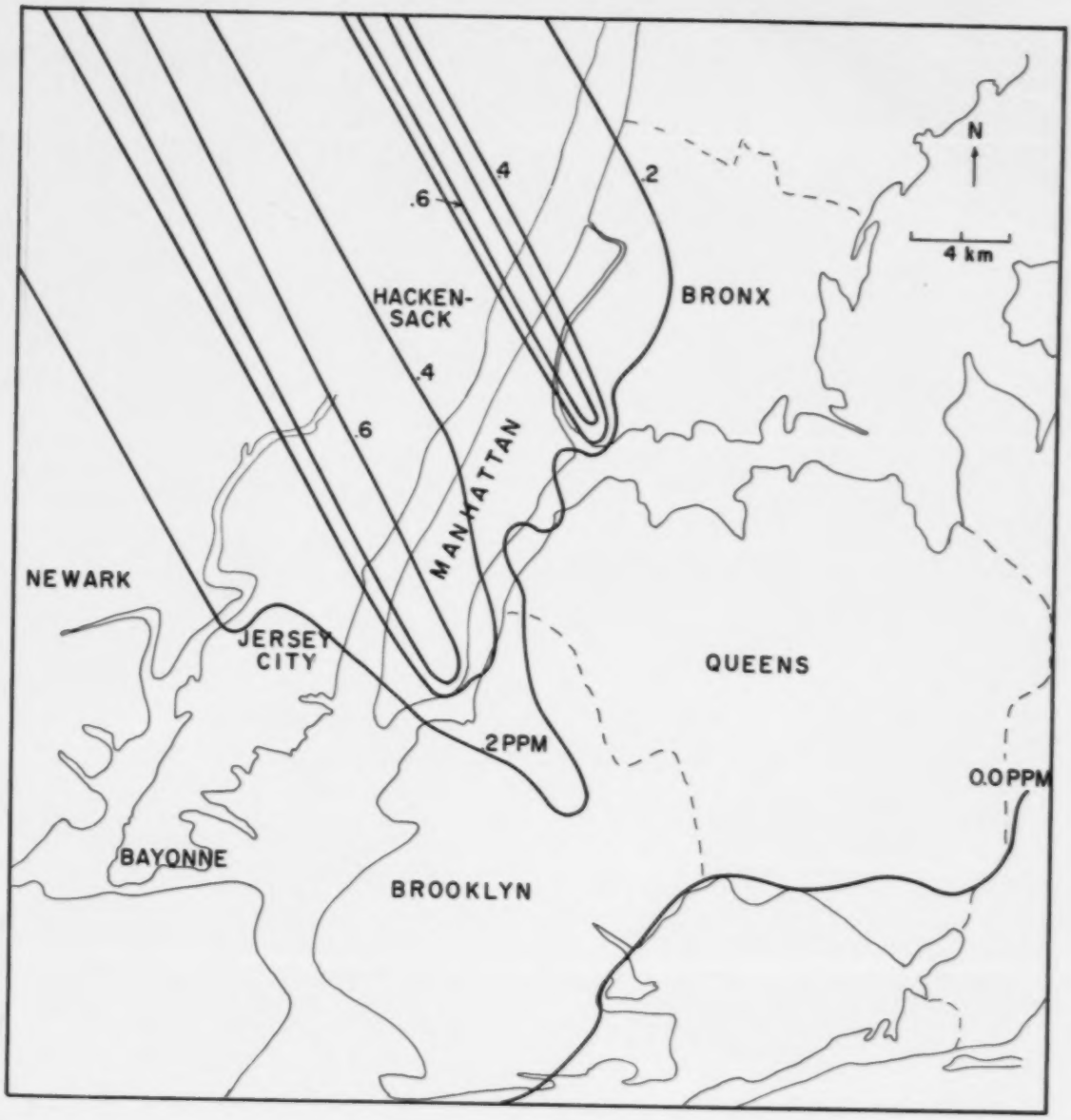

Figure 17. Predicted isopleth pattern of SO_2 mixing ratio (ppm) in the area of Manhattan Island for the period 0630-0930 EST, 16 November 1966.

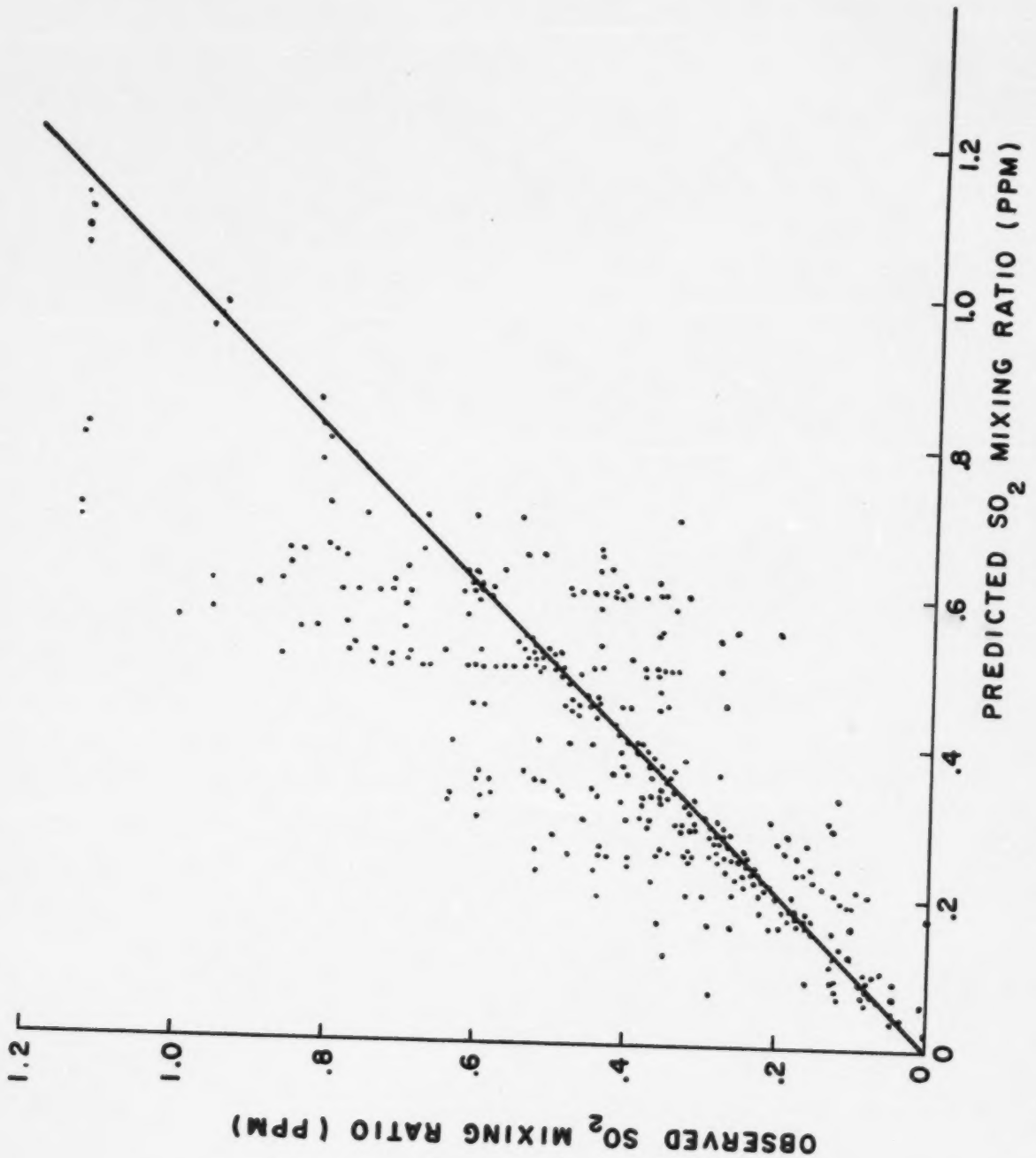

Figure 18. A plot of the observed against predicted SO_2 mixing ratio. The solid line is the theoretical one to one relation.

ter and from 9 fixed observation sites operated by New York City. The overall standard error was .13 ppm and the linear correlation coefficient was .84. Statistics for the individual studies are shown in Table IV.

Table IV. Statistics showing the differences between the observed and predicted values of m.

Time (EST)	Number of Observations	Observed Averaged Value of m(ppm)	Averaged Predicted value of m(ppm)	Standard Error (ppm)
9 March 1966 0630-0800	64	.51	.52	.16
10 March 1966 0600-1000	107	.40	.42	.10
11 March 1966 0630-0730	46	.39	.44	.15
3 May 1966 0600-0700	51	.39	.38	.15
16 November 1966 0630-0930	120	.37	.33	.12
Total	388	.42	.40	.13

More support for the validity of our air pollution model is presented in Figure 19. This shows the values of m observed during automobile traverses across the center of Manhattan Island. The theory reproduces the general features in a convincing manner.

The air pollution model is based upon the assumption that the pollutant is homogeneously distributed in the vertical within the mixing layer. It is of interest to inquire how the model predicts the pollution which was actually observed at the ground sites. As shown in Figure 20 the agreement is still very good. The mean observed and predicted values of m were .41 and .40 ppm respectively. The standard error of estimate was .11 ppm. Such agreement is comparable to that presented in Figure 18.

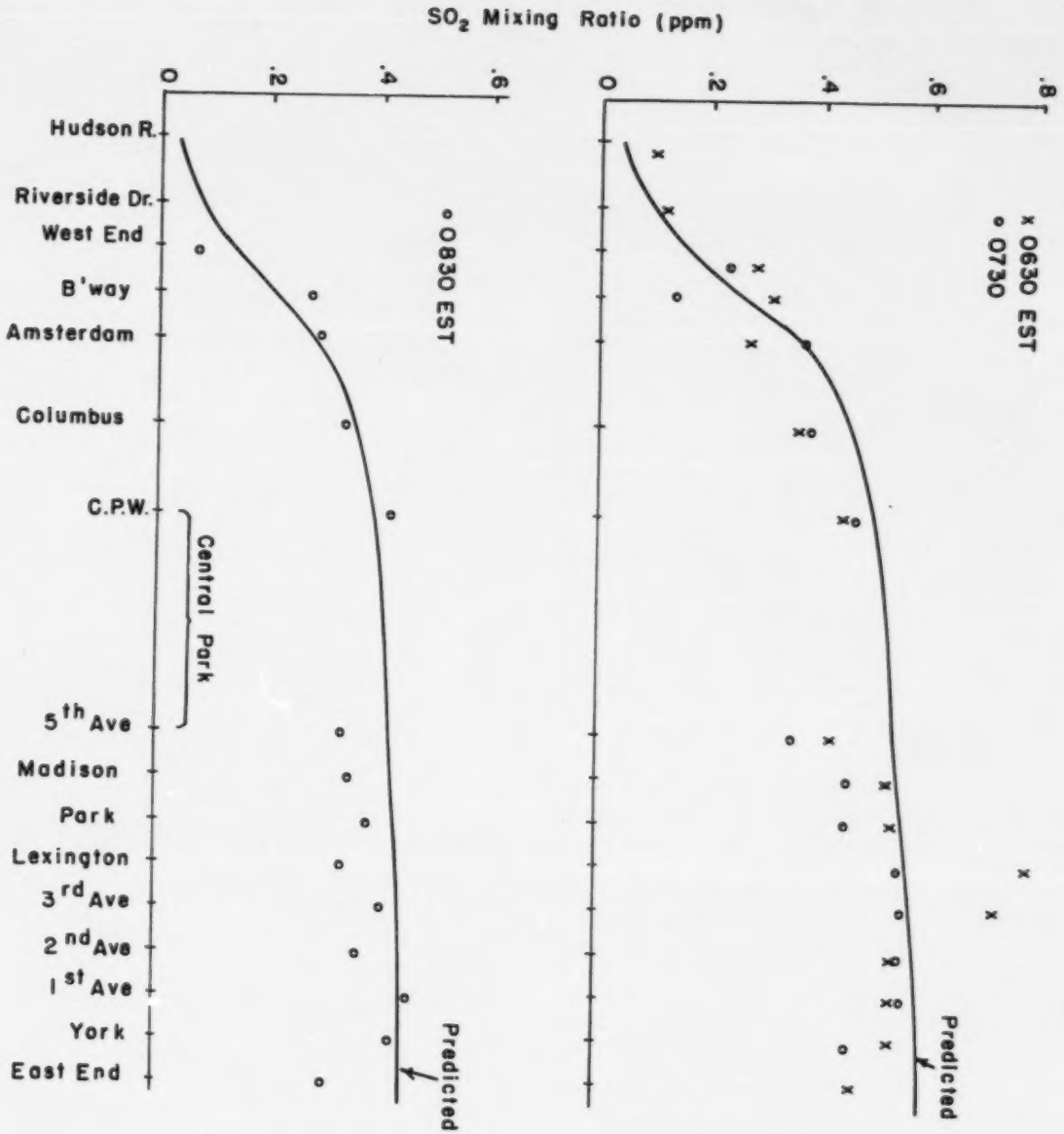

Figure 19. Observed and predicted variation of SO_2 in a NW-SE section through 79th Street, Manhattan.

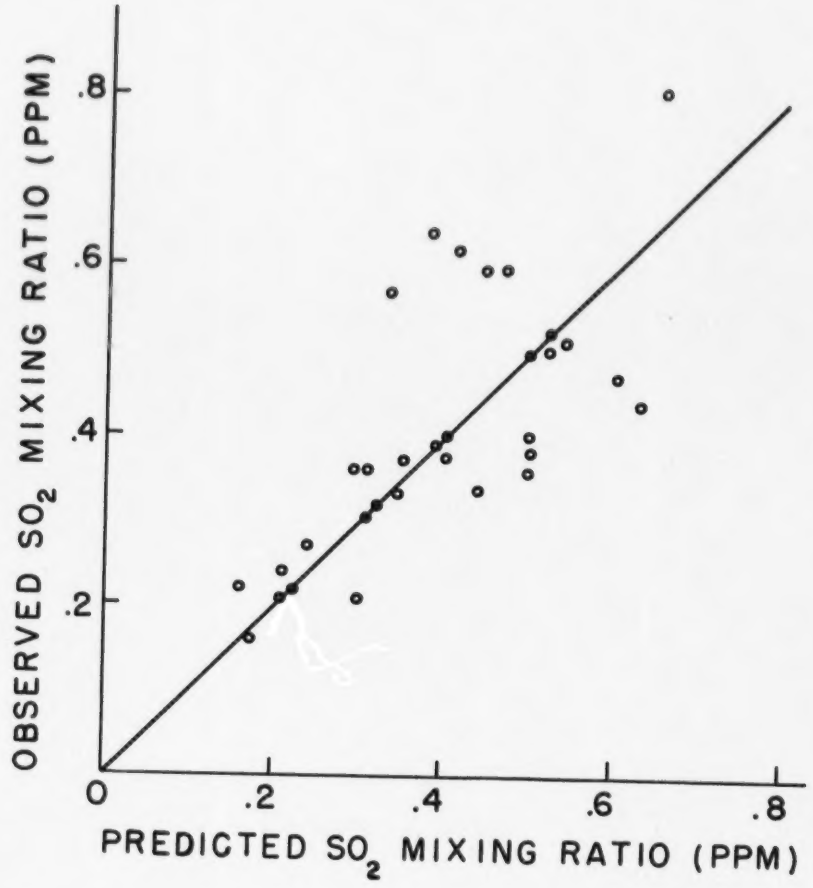

Figure 20. A verification of the model against SO_2 mixing ratios observed at ground based stations. The solid line is the theoretical one to one relation.

(iv) The urban heat island under calm conditions

We have been examining the urban heat island under conditions of non-zero wind. There are no data available for testing the model under calm conditions. But it is nonetheless of interest to examine the predictions of the urban heat island model under calm conditions, especially where the predictions apply to air pollution. These predictions are of particular interest because a unique feature of the pollution model advanced in this paper is its ability to predict the distribution of pollutants under calm conditions.

Equations (21) and (26) can be used to forecast the depth of the mixing layer and the variation of pollution for a hypothetical calm. It is proposed to examine the effect a sudden onset of a calm would have upon the distributions of h and m for 10 March 1966. Beginning with the fields of h and m shown in Figures 13 and 16 for 0700, calculations were performed to predict the distributions after two hours of calm. The results of these calculations are given in Figures 21 and 22.

As expected, the duration of the calm has spectacular effects upon the depth of the mixing layer. The effects of local heating in Elizabeth, Newark, Jersey City as well as Manhattan, Brooklyn and the Bronx are readily detectable. In portions of these cities the two hour calm causes an increase in depth of the mixing layer by amounts in excess of 150 m.

The most significant effect of the calm is shown in the distribution of pollutants. Without horizontal ventilation pollutants remain in their region of origin. Figure 22 shows very large mixing ratios over the built-up cities. In some of the areas the level of pollution is predicted to increase

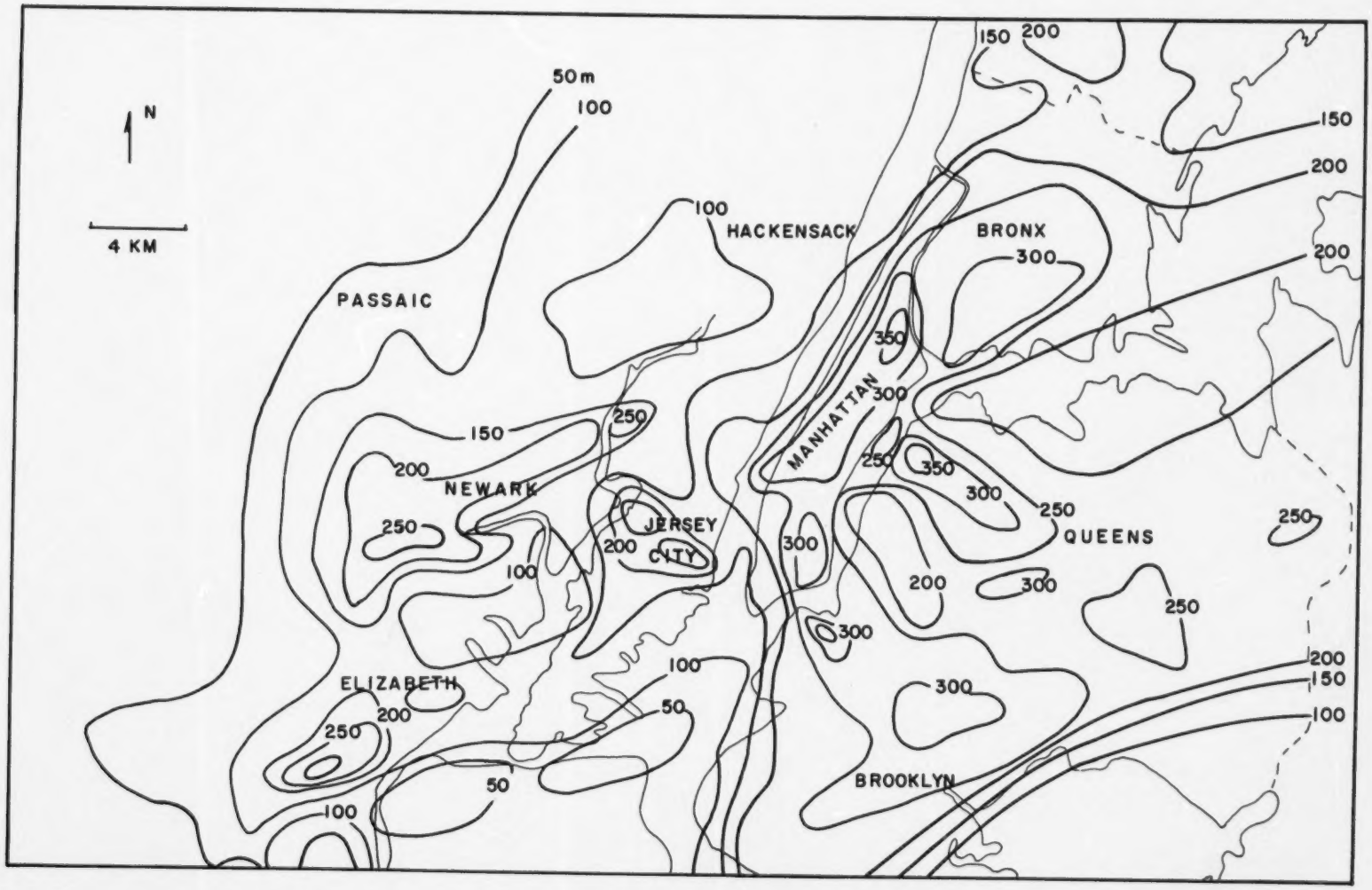

Figure 21. The distribution of the height of the elevated stable layer for the morning of 10 March 1966 following a hypothetical calm period of 2 hours duration.

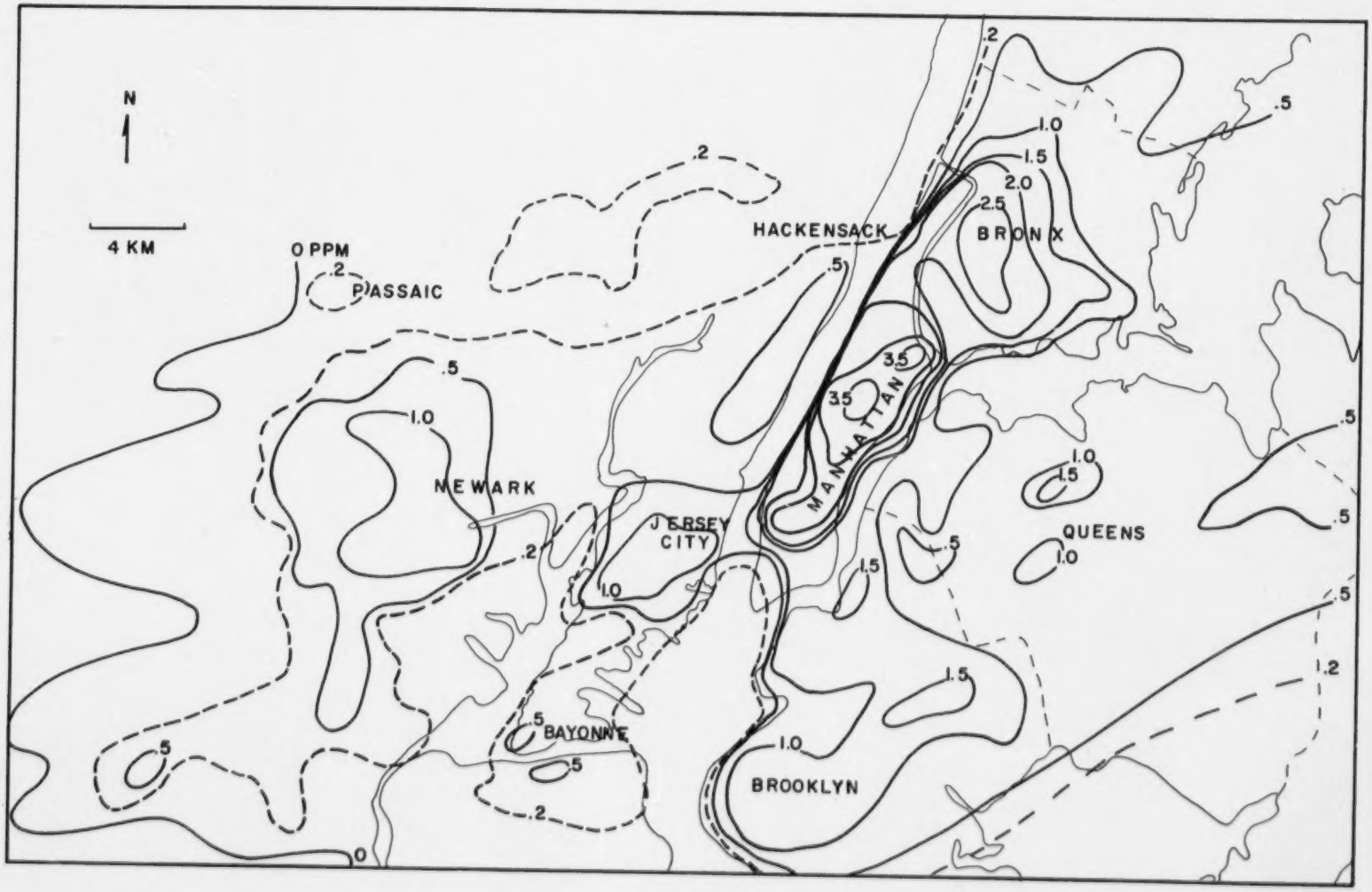

Figure 22. Isopleth pattern of SO_2 mixing ratio (ppm) for the morning of 10 March 1966 following a hypothetical calm period of 2 hours duration.

by more than 500%. Fortunately, calms are not a common feature of New York's wind climatology and when they do occur they seldom last much more than an hour.

XIV. The Urban Heat Island in Summer

(i) Estimates of Q_{G_1}

Most of the temperature soundings available from the Urban Air Pollution Dynamics Study were made from mid-September to mid-May. The only summer soundings which show a well developed inversion were made from 0430 to 0600 EST 16 July 1964. They can be used to provide first estimates of the amount of heat released in the early morning from the pavement and concrete of New York City.

Lettau (1951) has shown that the release of stored solar heat from a material at a given time of day is proportional to the amplitude of the diurnal temperature wave $\Delta T(°C)$. If we assume that the quantity of concrete and asphalt in a square mile is proportional to N, the number of housing units (h.u.), then

$$Q_{G_1} = \frac{kN\Delta T}{d} \qquad (27)$$

where

k = proportionality constant which will be a function of the time of day

d = a conversion factor which makes the equation dimensionally correct

In the early hours of the July morning during which time our soundings were made, heat release from industrial sources, domestic heating units, and vehicular activity should be negligible. Therefore from equations (4) and (15)

$$h^2 = \frac{2}{c_p \rho U \alpha} \int_{x_1}^{x} \left(Q_{G_1} - \sigma(T_1^4 - T_0^4) - Q_{S_0} \right) dx$$

Now with expression(27) and some manipulations.

$$k = \frac{d}{\Delta T \int_{x_1}^{x} N \, dx} \left(\frac{c_p \rho U \alpha h^2}{2} + \int_{x_1}^{x} (\sigma(T_1^4 - T_0^4) + Q_{S_0}) \, dx \right)$$

With observed values of h and a knowledge of the parameters on the right hand side of the above equation one can estimate k and thence Q_{G_1}.

For the morning of 16 July 1964 ΔT had the value of 4.5 °C. From this information together with that 16 July data listed in Table II, an average value for k of 1.1×10^{-4} units was calculated. The resulting estimates of Q_{G_1} derived from equation (27) are presented in Figure 23. On the basis of this figure one sees that less than one-half as much heat was released by the city as during an average winter morning (Figure 11).

Data concerning the depth of the mixing layer from other soundings obtained during the summer can be used to check the values of Q_{G_1} derived from equation (27). Such data are available from soundings made over New York City from 0430-0600 EST 22 June 1966 as part of a project

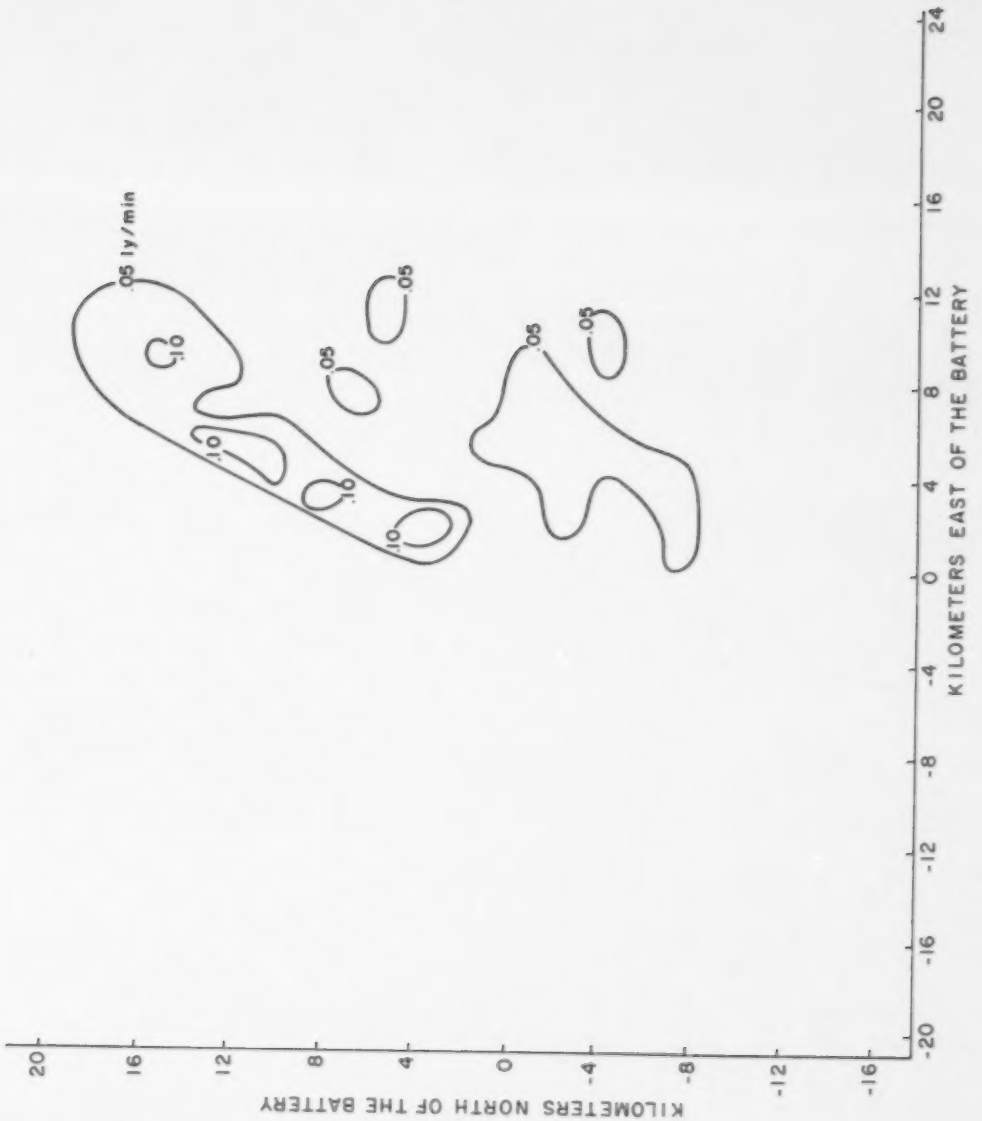

Figure 23. Predicted isopleths of heat release (ly/min) from pavement and concrete for the period 0430-0600 EST, 16 July 1964.

sponsored by Consolidated Edison Company (Simon, 1968). The amplitude of the diurnal temperature wave was 5.9°C. The remaining 22 June 1966 data are given in Table II.

Figure 24 shows the good agreement between the predicted and observed depths of the mixing layer. The figure also displays the observed mixing depths for the 16 July 1964 period from which the value of k was deduced.

(ii) Variation of m

Much of the fuel burnt during the summer by residential units for heating hot water and cooking is not available for increasing the thickness of the mixing layer. Rather much of the heat is yielded to sewers and from thence to nearby rivers. But the SO_2 released by the fuel is still conducted to the atmosphere. If it were not for the heat released from pavement and concrete which acts to deepen the mixing layer, the elevated stable layer would be closer to the ground and pollution levels could become very high.

Figure 25 shows the predicted variation of m over the New York City area for the early morning of 16 July 1964. It is based on the assumption that 20% of the annual fuel consumption is used for heating hot water and for cooking. As may be seen, the levels of pollution are much lower than during the non-summer days we have examined.

Unfortunately, helicopter data are not available for testing the distribution shown in Figure 25. The information attainable from the few available fixed sampling sites is not conclusive.

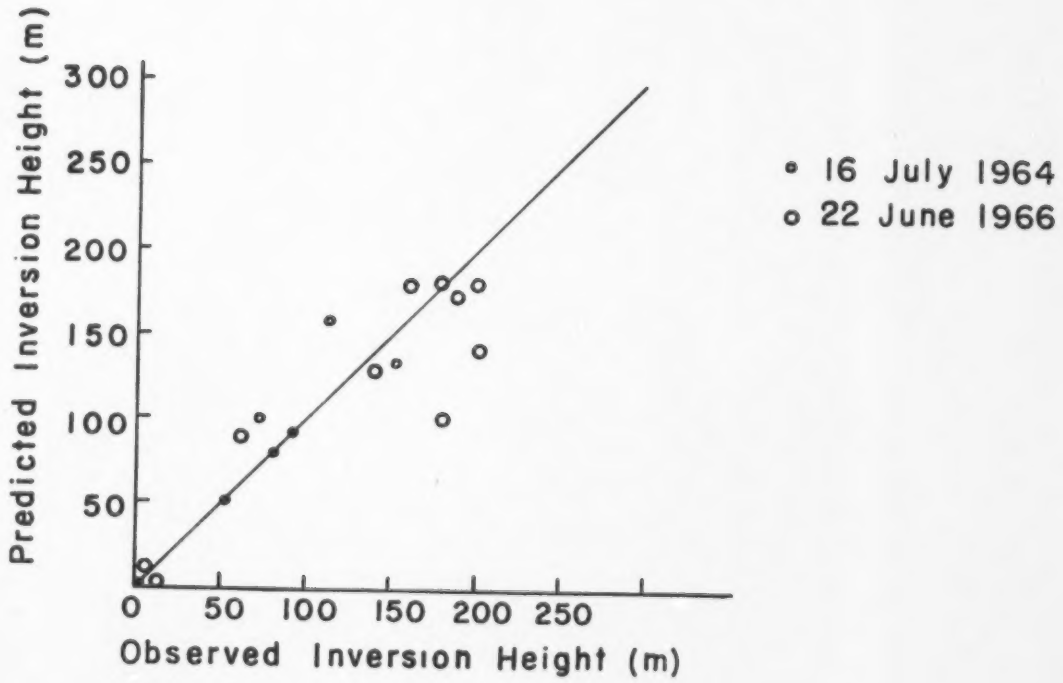

Figure 24. A plot of the observed against predicted inversion heights for the two summer study periods. The solid line depicts the theoretical one to one relation.

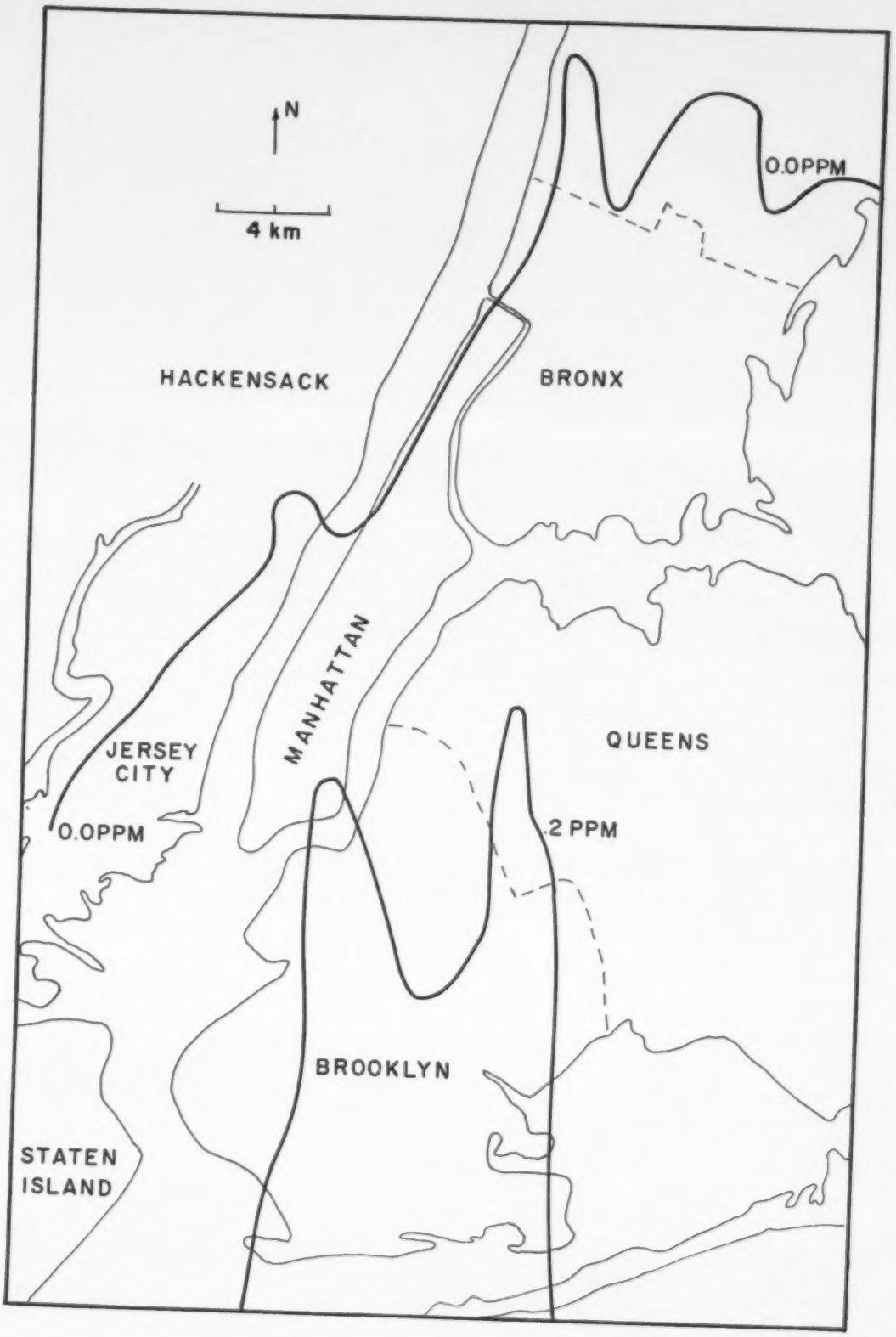

Figure 25. Predicted variation of m over the New York area for the early morning of 16 July 1964.

XV. Conclusions

The model for the urban heat island presented in this paper has several serious defects. It cannot for instance accommodate the complex mesoscale wind patterns which often exist at low wind speeds. Nor does it accommodate the non-steady state features of the air's stability and of the heat sources. Perhaps its greatest disappointment lies in its failure to explicate a detailed vertical temperature profile downwind of the urban heat island. Because of these defects it is questionable whether the present model is applicable over distances in excess of 50 km or over time scales in excess of ten hours.

Despite the above shortcomings of the simple thermodynamic model, it has achieved notable successes with six facets of the urban heat island phenomena. The achievements of the model are as follows:

(1) It provides a basis for defining the urban heat island.

(2) It accounts in a general manner for the surface isotherm pattern associated with urban heat islands and also for the ground based layer of stable air found downwind of urban heat islands.

(3) It accurately predicts the depth of the mixing layer.

(4) In conjunction with measurements of vertical temperature profiles it provides a means of roughly estimating the heat release from the concrete and pavements of a city during summer months.

(5) It accurately predicts the variation of pollution within the urban heat island.

(6) It provides the only means of calculating the variation of pollution

during periods of calm.

It should be understood that the model does not yet provide a tool for forecasting air pollution. Its use for such purposes must await a means of predicting the parameter α. This quantity is determined by the little understood processes of heat exchange between stable air and the ground.

References

Balchin, W.G.V. and N. Pye, 1947: A micro-climatological investigation of Bath and the surrounding district. Q.J.R.M.S., 73, p. 297.

Berljand, M.E., 1968: Meteorological factors determining the dispersion of atmospheric pollutants under urban conditions. Presented at the WHO/WMO Symposium on Urban Climates and Building Climatology. Brussels 15-25 October 1968.

Blackwell, M.J., R.H. Eldridge and G.D. Robinson, 1954: Estimation of the reflection and absorption of solar radiation by a cloudless atmosphere from recordings at the ground with results from Kew Observatory. Report No. 894, 11 p., Air Ministry, London.

Bornstein, R.D., 1968: Observations of the urban heat island effect in New York City. J. Applied Meteorology, 7, pp. 575-582.

Chandler, T.J., 1962: London's urban climate. Geog. J., 127, pp.279-302.

_____, 1965: The Climate of London. London, Hutchinson, p.292.

_____, 1967: Absolute and relative humidities in towns. Bull. Amer. Met. Soc., 48, pp. 394-399.

Clarke, J.F., 1969: Nocturnal urban boundary layer over Cincinnati, Ohio. Mon. Wea. Rev., Vol. 97, No. 8, pp. 582-589.

Davidson, B., 1967: A summary of the New York Urban Air Pollution Dynamics Research Program. J. Air Pollution Control Assoc.,

DeMarrais, G.A., 1961: Vertical temperature differences observed over an uran area. Bull. Amer. Met. Soc., 42, pp. 548-554.

Duckworth, F.S. and J.S. Sandberg, 1954: The effects of cities upon horizontal and vertical temperature gradients. Bull. Amer. Meteor. Soc., 35, pp. 198-207.

East, C.C., 1968: Total solar radiation recorded in Montreal and in the countryside. Paper presented to the Second Annual Congress of the Canadian Met. Soc. Colgary, 3-5 June 1968.

Fuggle, R.F. and T.R. Oke, 1968: Infrared flux divergence and the urban heat island. Presented at the WHO/WMO Symposium on Urban Climates and Building Climatology, Brussels, 15-25 October 1968.

Haltiner, G.J. and F.L. Martin, 1957: Dynamical and Physical Meteorology. McGraw-Hill Book Co., Inc., New York, p. 253.

Hammon, W.H. and F.W. Duenchel, 1902: Abstract of a comparison of the minimum temperatures recorded at the U.S. Weather Bureau and the Forest Park Meteorological Observatories, St. Louis, Missouri, for the year 1891. Mon.Wea. Rev., 30, p. 11.

Hand, I.F., 1943: Transmission of the total and the infrared component of solar radiation through a smoky atmosphere. Bull. Amer. Met. Soc., 24, pp. 201-204.

Howard, L., 1833: Climate of London Deduced from Meteorological Observations. Third Edition, London, Harvey and Darton.

Kratzer, P.A., 1956: The Climate of Cities (English translation of German Book), American Meteorological Society, Boston.

Kung, E.C., R.A. Bryson and D.H. Lenschow, 1964: Study of a continental surface albedo on the basis of flight measurements. Mon. Rev. Rev., 92, pp. 543-564.

Lettau, H., 1950: Theory of surface temperature and heat transfer oscillations near a level ground surface. Trans. Amer. Geophys. Union, 32, pp. 189-200.

London, J., 1957: A study of the atmospheric heat balance. Final Report, Project No. 131, Contract No. AF 19 (122-165) New York University.

Middleton, W.E.K. and F.G. Millar, 1936: Temperature profiles in Toronto. J. Roy. Ast. Soc. (Toronto), 30, p. 265.

Mitchell, J.M., 1962: The thermal climate of cities, Symposium, Air Over Cities, Public Health Service, SEC Technical Report A62-5, pp. 131-145.

Munn, R.E., 1966: Descriptive Micrometeorology. Academic Press, New York, p. 245.

Reichel, E., 1933: An example of great temperature differences between town and county station. Preussisches Meteorologisches Institut. Veroffentlichungen, Bericht, No. 402, p. 72.

Renou, E., 1862: Differences de temperature entre Paris et Choisyle-Roi. Soc. Met. de France, 10, p. 105.

Schmidt, W., 1929: Distribution of minimum temperatures during the frost night of 12 May 1927 within Vienna. Fortschritte der Landwistschoft.

Sheppard, P.A., 1958: The effect of pollution on radiation in the atmosphere. Int. J. Air Water Poll., 1, pp. 31-43.

Shuleikin, V.V., 1953: Molecular Physics of the Sea. Trans. U.S. Navy Hydrographic Office.

Simon, C.S., 1968: Plume rise and plume concentration distribution from Consolidated Edison Plants in New York City. Final Report, Geophysical Sciences Laboratory, Technical Report No. 68-15, New York University.

Summers, P.W., 1965: An urban heat island model, its role in air pollution problems with application to Montreal. Presented at the First Canadian Conference on Micrometeorology, Toronto, 12-14 April 1965.

Sundborg, A., 1950: Local climatological studies of the temperature conditions in an urban area. Tellus, 2, pp. 222-232.

U.S. Department of Commerce, 1960: Surface water temperature and salinity Atlantic Coast, North and South America. Coast and Geodetic Survey, Publication 31-1.

Vowinckel, E. and B. Taylor, 1965: Evaporation and sensible heat flux over the Arctic Ocean. Arch. Met. Geoph. Biokl., B14, pp. 36-52.

Whiten, A.J., 1956: The ventilation of Oxford circus. Weather, Vol. 11, pp. 227-229.